



Title	Structural insights into the substrate stereospecificity of D-threo-3-hydroxyaspartate dehydratase from <i>Delftia</i> sp HT23: a useful enzyme for the synthesis of optically pure L-threo- and D-erythro-3-hydroxyaspartate
Author(s)	Matsumoto, Yu; Yasutake, Yoshiaki; Takeda, Yuki; Tamura, Tomohiro; Yokota, Atsushi; Wada, Masaru
Citation	Applied microbiology and biotechnology, 99(17), 7137-7150 https://doi.org/10.1007/s00253-015-6479-3
Issue Date	2015-09
Doc URL	http://hdl.handle.net/2115/62880
Type	article (author version)
File Information	70914(Wada).pdf



[Instructions for use](#)

1 **Structural insights into the substrate stereospecificity of**
2 **D-threo-3-hydroxyaspartate dehydratase from *Delftia* sp. HT23: a useful**
3 **enzyme for the synthesis of optically pure L-threo- and**
4 **D-erythro-3-hydroxyaspartate**

5
6 Yu Matsumoto,^a Yoshiaki Yasutake,^{b*} Yuki Takeda,^a Tomohiro Tamura,^b Atsushi Yokota,^a and
7 Masaru Wada^{a*}

8
9 ^aLaboratory of Microbial Physiology, Research Faculty of Agriculture, Hokkaido University,
10 Kita-9, Nishi-9, Kita-ku, Sapporo 060-8589, Japan, and ^bBioproduction Research Institute,
11 National Institute of Advanced Industrial Science and Technology (AIST), 2-17-2-1
12 Tsukisamu-Higashi, Toyohira-ku, Sapporo 062-8517, Japan

13
14 *Corresponding authors

15 Tel: +81-11-857-8514; Fax: +81-11-857-8980; E-mail: y-yasutake@aist.go.jp

16 Tel: +81-11-706-4185; Fax: +81-11-706-4961; E-mail: wada@chem.agr.hokudai.ac.jp

17
18 **Key words:** D-threo-3-hydroxyaspartate dehydratase, *Delftia* sp. HT23, alanine racemase,
19 pyridoxal 5'-phosphate, enzymatic optical resolution

1 Abstract

2 **D-threo-3-hydroxyaspartate dehydratase (D-THA DH) is a fold-type III pyridoxal**
3 **5'-phosphate-dependent enzyme, isolated from a soil bacterium of *Delftia* sp. HT23. It**
4 **catalyzes the dehydration of D-threo-3-hydroxyaspartate (D-THA) and**
5 **L-erythro-3-hydroxyaspartate (L-EHA). To elucidate the mechanism of substrate**
6 **stereospecificity, crystal structures of D-THA DH were determined in complex with**
7 **various ligands, such as an inhibitor [D-erythro-3-hydroxyaspartate (D-EHA)], a**
8 **substrate (L-EHA), and the reaction intermediate (2-amino maleic acid). The C^β-OH of**
9 **L-EHA occupied a position close to the active site Mg²⁺, clearly indicating a possibility of**
10 **metal-assisted C^β-OH elimination from the substrate. In contrast, the C^β-OH of an**
11 **inhibitor was bound far from the active site Mg²⁺. This suggests that the substrate**
12 **specificity of D-THA DH is determined by the orientation of the C^β-OH at the active site,**
13 **whose spatial arrangement is compatible with the 3R configuration of**
14 **3-hydroxyaspartate. We also report an optically pure synthesis of**
15 **L-threo-3-hydroxyaspartate (L-THA) and D-EHA; promising intermediates for the**
16 **synthesis of β-benzyloxyaspartate, by using a purified D-THA DH as a biocatalyst for the**
17 **resolution of racemic DL-THA and DL-EHA. Considering 50% of the theoretical**
18 **maximum, efficient yields of L-THA (38.9%) and D-EHA (48.9%) as isolated crystals**
19 **were achieved with >99% enantiomeric excess (*e.e.*). The results of nuclear magnetic**
20 **resonance signals verified the chemical purity of the products. We were directly able to**
21 **isolate analytically pure compounds by the recrystallization of an acidified reaction**
22 **mixtures (pH 2.0), and thus avoiding the use of environmentally harmful organic**
23 **solvents for the chromatographic purification.**

24

25

1 **Introduction**

2 3-Hydroxyaspartate and its derivatives have attracted attention because of their
3 biological activity as competitive blockers against glutamate transporters [Excitatory Amino
4 Acid Transporters 1-5 (EAAT1-5)] in the mammalian central nervous system (Arriza et al.
5 1994; Arriza et al. 1997; Shimamoto et al. 1998; Shimamoto et al. 2004; Shimamoto 2008).
6 3-Hydroxyaspartate has two chiral centers and thus it exhibits four stereoisomers, namely
7 *D-threo*-3-hydroxyaspartate (2*R*,3*R*; D-THA), *L-threo*-3-hydroxyaspartate (2*S*,3*S*; L-THA),
8 *D-erythro*-3-hydroxyaspartate (2*R*,3*S*; D-EHA) and *L-erythro*-3-hydroxyaspartate (2*S*,3*R*;
9 L-EHA) (Fig. 1). Recently, we have identified and cloned a gene encoding D-THA
10 dehydrating enzyme (D-THA DH) from a soil bacterium *Delftia* sp. HT23 (Maeda et al. 2010).
11 D-THA DH displays a preference for the dehydration of D-THA and L-EHA, and is only
12 slightly active against L-THA, while showing no activity on D-EHA. Although, there are
13 several reported enzymes that act on 3-hydroxyaspartate (Wada et al. 1999; Liu et al. 2003;
14 Wada et al. 2003; Murakami et al. 2009), D-THA DH is the only enzyme known to exhibit an
15 efficient dehydratase activity towards D-THA. Thus, this enzyme was assigned a new Enzyme
16 Commission (EC) number as 4.3.1.27.

17 We have also found that D-THA DH belongs to a fold-type III group of pyridoxal
18 enzymes of which bacterial alanine racemases are the typical members (Schneider et al. 2000;
19 Eliot and Kirsch 2004). Our previous work revealed that D-THA DH contains a pyridoxal
20 5'-phosphate (PLP) as its cofactor but its racemization activities on alanine, serine and
21 aspartate were below the detection limit. To date, many crystal structures of alanine racemases
22 from diverse bacteria have been deposited in the Protein Data Bank (PDB). Nevertheless,
23 very little is known about the structure of dehydratases whose predictive structure closely
24 resembles that of alanine racemases. Eukaryotic D-serine dehydratase has been recently
25 identified as a common member of the fold-type III group of pyridoxal enzymes (Ito et al.
26 2008; Tanaka et al. 2008). D-THA DH shows amino acid sequence similarity (26-36%) with

1 D-serine dehydratases derived from *Saccharomyces cerevisiae* (scDSD; Ito et al. 2008) and
2 chicken kidney (chDSD; Tanaka et al. 2008). The crystal structure of chDSD complexed with
3 D-serine has been previously reported (Tanaka et al. 2011); however, no structural information
4 is available regarding 3-hydroxyaspartate-recognition mechanism of this enzyme family.

5 Various effective methods for the preparation of 3-hydroxyaspartate as a racemate or
6 an individual stereoisomer have been reported (Kaneko and Katsura 1963; Antolini et al.
7 1997; Cardillo et al. 1999; Khalaf and Datta 2008). It is of notable interest to develop a
8 synthesis method for L-THA due to the obvious demand for its derivative
9 *L-threo-β*-benzyloxyaspartate (L-TBOA) in the field of neuroscience as a potent blocker of
10 EAAT subtypes (Shigeri et al. 2004; Shimamoto 2008). L-THA acts as a high-affinity
11 substrate for EAAT1-4 and as an inhibitor for EAAT5, thus providing a suitable lead
12 compound as a blocker of EAATs (Arriza et al. 1994; Arriza et al. 1997; Shigeri et al. 2001).
13 Most of the L-THA synthetic routes relying on the chemical methods utilize a chiral template
14 such as *trans*-methyl cinnamate as a starting material (Deng et al. 1995; Bionda et al. 2012).
15 However, these routes require several reaction steps and are time-consuming. In contrast to
16 the synthetic chemistry approach, few bacterial enzymes are known to efficiently produce
17 L-THA. Strieker et al. (2008) have reported the bioconversion of L-aspartate to L-THA by
18 using a single mutant of asparagine oxygenase (AsnO_{D241N}) from *Streptomyces coelicolor*.
19 However, the activity and the thermal stability of AsnO_{D241N} were found to be lower than
20 those of AsnO_{WT}. Alternatively, Hara and Kino (2010) have reported a more efficient L-THA
21 bioconversion by overexpression of native AsnO using *Escherichia coli*, coupled with *E. coli*
22 asparaginase *in vivo*. Optically pure 3-hydroxyaspartate production by using a simple strategy
23 is still a challenging process in both synthetic and biological chemistry. While many groups
24 have attempted to increase the productivity, a dramatic improvement in the efficiency has not
25 been realized, resulting in L-THA being an expensive product.

26 In this paper, we present crystal structures of D-THA DH complexed with its inhibitor

1 D-EHA, a poorly active H351A mutant complexed with its substrates L-EHA, and H351A
2 mutant complexed with the reaction intermediate 2-amino maleic acid. High-resolution
3 structures provide a clear picture of how substrate/inhibitor binds to the enzyme, allowing us
4 to propose a model for the catalytic reaction as well as the mechanism for the substrate
5 stereospecificity of D-THA DH. We also report an enzymatic optical resolution by using
6 purified D-THA DH, and show efficient yields of L-THA and D-EHA as isolated crystals with
7 high enantiomeric excess (*e.e.*). This novel approach for the production of optically pure
8 3-hydroxyaspartate is simple, environment friendly and is applicable for the large-scale
9 production.
10
11

1 **Materials and methods**

2

3 **Materials**

4 Oligonucleotides were obtained from Eurofins Genomics, Inc. (Tokyo, Japan). A
5 (±)-*trans*-epoxysuccinic acid and DL-*threo*-3-hydroxyaspartate (DL-THA) were purchased
6 from Tokyo Chemical Industry Co., Ltd. (Tokyo, Japan). L-EHA was purchased from Wako
7 Pure Chemical Industries, Ltd. (Osaka, Japan). An isolated strain, identified as *Delftia* sp.
8 HT23, has been deposited in the AHU Culture Collection of Hokkaido University under
9 accession number AHU2003.

10

11 **Site-directed mutagenesis**

12 Plasmids expressing the H351A and C353A mutants were constructed using inverse
13 PCR method with a KOD-Plus-Mutagenesis Kit (Toyobo Co., Ltd., Osaka, Japan) according
14 to the manufacturer's instructions. Previously described D-THA DH expression vector served
15 as a template DNA (Matsumoto et al. 2013). Following synthetic oligonucleotide primers
16 were used: H351A forward, 5'-**GCCG**CCTGCGCCACGGGCGCGCAGTTC-3', and reverse,
17 5'-GTTGGGCAGGATGCGCAGCCGCGTGCC-3'; C353A forward,
18 5'-**GCCG**CCACGGGCGCGCAGTTCCCGGCC-3', and reverse,
19 5'-GGCATGGTTGGGCAGGATGCGCAGCCG-3'. The bold bases encode an Ala residue
20 instead of His351 and Cys353, respectively. The inverse PCR conditions were as follows:
21 initial 2-min denaturation at 94 °C, followed by 10 cycles of amplification at 98 °C for 10 s
22 and at 68 °C for 5 min. The nucleotide substitutions were confirmed by DNA sequencing. The
23 nucleotide sequence of the gene encoding D-THA DH from *Delftia* sp. HT23 has been
24 deposited in the DDBJ/EMBL/GenBank database under the accession number AB433986.
25 Each mutant was expressed in *Rhodococcus erythropolis* L88 cells according to a previously
26 described method (Nakashima and Tamura 2004a,b).

1
2
3
4
5
6
7
8
9
10
11
12
13
14
15
16
17
18
19
20
21
22
23
24
25
26

Recombinant protein expression and purification

The recombinant enzymes used in this work contained additional Met-Gly-(His)₆-Ala-Met-Ser residues at the N-terminus. Recombinant D-THA DH and its mutants were overproduced using a *R. erythropolis* expression system and purified by Ni-affinity chromatography, as described previously (Matsumoto et al. 2013). The fractions containing recombinant proteins were collected, dialyzed against the buffer (10 mM Tris-HCl pH 8.0, 0.01 mM PLP, and 0.1 mM dithiothreitol), and subsequently concentrated to 15 mg mL⁻¹ using a centrifugal filtration device (10,000 Da molecular-weight cutoff, Merck Millipore, Ltd., Darmstadt, Germany). Protein concentrations were determined by the Bradford method using the Bio-Rad protein assay (Bio-Rad Laboratories, Inc., Hercules, CA) with bovine serum albumin as a standard. Protein purity was checked using SDS-PAGE (Fig. S1).

Crystallization and X-ray diffraction studies

All crystallization experiments were performed at 20 °C by using either sitting drop or hanging drop vapor-diffusion method. The substrate-free wild-type enzyme was crystallized as previously described (Matsumoto et al. 2013). For the preparation of the substrate/inhibitor complex, the purified sample was mixed with molar excess of substrate/inhibitor (~50 mM) and incubated overnight before crystallization setup. All D-THA DH crystals used in this work were obtained in the solution consisting of 0.1 M Tris-HCl pH 8.5, 0.2 M MgCl₂, and 10-20% PEG 3350. Prior to X-ray diffraction studies, crystals were briefly soaked in a cryoprotectant solution containing a crystallization mother liquor and an additional 20% glycerol. For the structure analysis of a metal-free enzyme, the crystals were briefly soaked in the Mg²⁺-free cryoprotectant solution consisting of 0.1 M HEPES-NaOH pH 8.0, 2.0 M ammonium formate, and 25% glycerol. Crystals were flash-cooled in a cold nitrogen gas stream or directly in the

1 liquid nitrogen. X-ray diffraction data were collected using a Charge Coupled Device (CCD)
2 detector (ADSC) at the Photon Factory (PF; Tsukuba, Japan). Raw diffraction images were
3 processed with the program iMosflm/SCALA (Battye et al. 2011; Winn et al. 2011) or
4 HKL2000 suite (Otwinowski and Minor 1997).

5

6 **Structure solution and model refinement**

7 The structure of D-THA DH was solved by a single-wavelength anomalous diffraction
8 (SAD) method with bromide-soaked crystals as described (Matsumoto et al. 2013). Bromide
9 sites were determined using the program SHELXC/D (Sheldrick 2008). Density modification
10 and model building were performed using the program SOLVE/RESOLVE (Terwilliger and
11 Berendzen 1999; Terwilliger 2000). Model refinement was performed using the program
12 REFMAC 5 (Murshudov et al. 2011), and the manual model fitting was done with the
13 program Coot (Emsley and Cowtan 2004). Ligand models not found in the Chemical
14 Component Dictionary were created using the program SKETCHER and the geometrical
15 restraints files were generated using the program LIBCHECK provided in the CCP4 program
16 package (Winn et al. 2011). Molecular drawings were prepared using the program PyMOL
17 (DeLano 2002). Atomic coordinates and the structure factor amplitudes of all the structures
18 reported in this paper were deposited in the RCSB Protein Data Bank under accession codes
19 3WQC, 3WQD, 3WQF, 3WQG, 4PB3, 4PB4, and 4PB5. Data collection and refinement
20 statistics are summarized in Table 1.

21

22 **Enzyme assay**

23 3-Hydroxyaspartate dehydratase activity was assayed spectrophotometrically by
24 measuring a change in the absorbance of NADH at 340 nm using a DU800 spectrophotometer
25 (Beckman Coulter, Inc., Brea, CA). Assay was performed using a coupling system with
26 NADH-dependent malate dehydrogenase (MDH), as described previously (Wada et al. 1999).

1 The standard assay mixture consisted of 100 mM Tris-HCl buffer (pH 8.0), 0.01 mM PLP, 0.1
2 mM MnCl₂, 10 mM D-THA or L-EHA as a substrate, 0.32 mM NADH, 10 units of MDH, and
3 an appropriate amount of the enzyme in a total volume of 0.5 mL. The reactions were carried
4 out at 30 °C with addition of the substrate. Reaction mixtures without substrate served as
5 controls. One unit of the enzyme is defined as 1 μmol of NADH utilized per minute at 30 °C
6 on the basis of an absorption coefficient of 6.22 mM⁻¹ cm⁻¹ at 340 nm.

7

8 **Chemical synthesis of DL-erythro-3-hydroxyaspartate**

9 DL-erythro-3-Hydroxyaspartate (DL-EHA) was synthesized by ammonolysis of a
10 (±)-*trans*-epoxysuccinic acid at 60 °C. Reaction product was evaporated to dryness, and the
11 resulting residue was dissolved in an acidified water (pH 2.0 adjusted with HCl). Water
12 solution was allowed to stand for 16 h at 4 °C. The appeared crystals of 3-hydroxyaspartate
13 were collected by filtration, washed with a small amount of the acidified water, and
14 subsequently dried in vacuum for 24 h. Resulting product was confirmed by thin layer
15 chromatography (TLC) and high performance liquid chromatography (HPLC) as described in
16 the analytical methods.

17

18 **Enzymatic optical resolution of DL-racemic 3-hydroxyaspartate**

19 Purified D-THA DH was used to prepare L-THA or D-EHA from the corresponding
20 racemates by an enzymatic optical resolution. The reaction mixture consisted of 100 mM
21 Tris-HCl buffer (pH 8.0), 0.01 mM PLP, 0.1 mM MnCl₂, 200 mM DL-THA or DL-EHA, and
22 purified D-THA DH in a total volume of 100 mL. Reactions were performed at 30 °C with
23 reciprocal shaking at a speed of 90 rpm and started by addition of 0.66 mg of the enzyme to
24 DL-THA solution and 0.87 mg to DL-EHA solution. Incubation was continued for 9 h or 12 h,
25 respectively. During incubation, D-form and L-form of 3-hydroxyaspartate in the reaction
26 mixture were monitored using HPLC and an amino-acid analyzer as described below.

1 Samples taken for the analyses were heated at 70 °C for 30 min to inactivate the enzyme.
2 After incubation, L-THA or D-EHA in the reaction product were isolated by crystallization as
3 described below.

4

5 **Isolation of L-THA or D-EHA**

6 The reaction product was acidified to pH 2.0 using HCl. Resulting solution was
7 evaporated to about 10 mL and subsequently allowed to stand for 16 h at 4 °C. Appeared
8 crystals of 3-hydroxyaspartate were collected with the same procedure as for the preparation
9 of DL-EHA. TLC, HPLC and nuclear magnetic resonance (NMR) spectroscopy as described
10 in the analytical methods, confirmed the resulting product.

11

12 **Analytical methods**

13 **TLC:** Crystallized DL-EHA, L-THA and D-EHA were confirmed by Silica Gel TLC
14 using 7:1:2 (v/v/v) ethanol/28% aqueous ammonia/water as a mobile phase. After developing
15 the TLC plates, compounds were visualized by using a Ninhydrin Spray (Wako Pure
16 Chemical Industries), followed by heating.

17 **HPLC:** For chiral analysis of amino acids, 2,3,4,6-tetra-*O*-acetyl- β -D-glucopyranosyl
18 isothiocyanate (GITC) was used for the amino acid derivatization. In a GITC derivatization
19 procedure, 0.1 mL of 0.2% (w/v) GITC (dissolved in acetonitrile) and 0.02 mL of 2% (v/v)
20 triethylamine (dissolved in water) were added to 0.01 mL of reaction samples that were
21 subsequently diluted with acetonitrile to make a total volume of 0.2 mL. The resulting
22 solution was allowed to stand for 30 min at 30 °C. The amino acid derivatives were analyzed
23 using HPLC at a flow rate of 1.0 mL min⁻¹ with a CAPCELL PAK C18 MGIII column (4.6 ×
24 250 mm; Shiseido Company, Ltd., Tokyo, Japan) at 40 °C. Thirty percent (v/v) methanol or
25 35% (v/v) methanol in water (pH 2.5 adjusted with H₃PO₄) were used as the mobile phases for
26 the analysis of DL-THA or DL-EHA, respectively. Detection was done with a UV detector

1 tuned at 250 nm. The enantiomeric excess (*e.e.*) was calculated from the peak areas of the
2 stereoisomers.

3 **Amino acid analyzer:** Total concentration of DL-THA or DL-EHA in the reaction
4 mixture was determined with a JLC-500S amino acid analyzer (JEOL, Ltd., Tokyo, Japan).

5 **NMR spectroscopy:** All NMR spectra were recorded on a Bruker AMX-500
6 spectrometer (Bruker Corporation, Billerica, MA, ¹H NMR: 500 MHz; ¹³C NMR: 125 MHz).
7 Samples taken for the analysis were dissolved in deuterium oxide (D₂O). Chemical shifts
8 were determined relative to the reference signal of an external
9 3-(trimethylsilyl)propionic-2,2,3,3-d₄ acid (TSP; δ_H, 0 ppm; δ_C, 0 ppm).

10

11

1 **Results**

2

3 **Overall structure of D-THA DH**

4 The crystal structure of D-THA DH was determined in the substrate-free form at a
5 resolution of 1.5 Å. The asymmetric unit comprises a dimer formed by a head-to-tail
6 association of two monomers (Fig. 2a). Each monomer is divided into N- and C-terminal
7 domains (Fig. 2b). The N-terminal domain (residues 17-257) consists of eight α -helices
8 ($\alpha 1$ - $\alpha 8$) and eight β -strands ($\beta 2$ - $\beta 9$) which constitute a well-known “TIM-barrel” fold,
9 providing a binding site for PLP. The first β -strand of the monomer, $\beta 1$, does not form the
10 TIM barrel and is a part of the C-terminal domain since $\beta 1$ is located at the extreme
11 N-terminus. The C-terminal domain, comprising of residues 1-16 and 258-380, is mainly
12 composed of β -strands. All the nine β -strands ($\beta 1$ and $\beta 10$ - $\beta 17$) of the domain form a β -sheet
13 in which the strands are arranged in an antiparallel orientation except for $\beta 1$ and $\beta 16$. This
14 β -sheet creates a six-stranded β -barrel structure in which the strands ($\beta 10$ - $\beta 11$ and $\beta 14$ - $\beta 15$)
15 are arranged in a Greek-key topology. The PLP-binding site is located at the center of the TIM
16 barrel, between two domains. The overall folding topology is typical of a bacterial alanine
17 racemase. Thus, the current structure provides a conclusive evidence that D-THA DH belongs
18 to the fold-type III group of pyridoxal enzymes.

19

20 **Cofactor binding site**

21 The active-site pockets harboring PLP are located at the dimer interface, between the
22 TIM barrel of one monomer and the C-terminal domain of the homodimeric partner.
23 Accordingly, residues bound to PLP (Lys43) yield two active sites per dimer. A highly defined
24 electron density was observed for the entire PLP molecule in each active site. The PLP
25 cofactor binds covalently *via* an imine bond to the ϵ -amino group of Lys43, forming an
26 internal aldimine (Schiff base) (Fig. 2c; Fig. S2a). The Lys residue is also highly conserved in

1 scDSD and chDSD (Ito et al. 2008; Tanaka et al. 2008). The internal aldimine and the
2 guanidine group of Arg141 are within hydrogen-bonding distance of the phenolic O atom of
3 PLP. The phosphate group of PLP is involved in forming hydrogen bonds to the side-chain
4 atoms of the residues Tyr177 and Thr218, and the main-chain atoms of the residues Thr218,
5 Gly236 and Val237. The pyridine ring of PLP makes a hydrogen bond between its nitrogen
6 atom and the guanidine group of Arg234.

7 We observed a strong electron density peak between side-chains of His351 and
8 Cys353 in each subunit. The electron density was assigned as fully occupied Mg^{2+} , and the
9 model was refined with the reasonable B-factor values comparable to those of nearby residues.
10 Mg^{2+} was probably bound due to the high concentration of $MgCl_2$ (200 mM) in the
11 crystallization solution. The metal-binding site is a part of the C-terminal domain and is
12 formed by His351 and Cys353, which coordinate the metal ion through the N- ϵ atom of the
13 imidazole ring and the thiol group, respectively (Fig. 2c; Fig. S2a). In addition to the two
14 residues, four water molecules complete the octahedral coordination of the Mg^{2+} . The PLP is
15 located near Mg^{2+} and its phosphate group lies at a distance of about ~ 5 Å from the metal
16 center. The sequence comparison of D-THA DH with scDSD and chDSD demonstrates that
17 the His and Cys residues coordinating the metal ion are well conserved in these proteins (Ito
18 et al. 2008; Tanaka et al. 2008). All the related proteins show a strong dependency on Zn^{2+} ,
19 while D-THA DH works with a various divalent cations including Mg^{2+} as discussed later (Fig.
20 S3).

21

22 **D-EHA (inhibitor) binding mode of D-THA DH**

23 Our previous work has revealed that the specific activity of D-THA DH towards
24 D-EHA is below the limits of detection. D-EHA inhibits D-THA DH with the K_i value of 0.114
25 mM, determined by replotting the slopes of the Lineweaver-Burk plots. Considering both the
26 results, it can be concluded that D-THA DH has a significant binding affinity towards D-EHA

1 but does not recognize it as a substrate. To elucidate how D-EHA binds in the active site of
2 D-THA DH, its structure was determined in the presence of D-EHA. The structure was
3 determined to a resolution of 1.5 Å and a clear electron density map was observed for the
4 whole D-EHA molecule bound to the PLP cofactor. The active site of each subunit includes a
5 D-EHA molecule and two Mg²⁺ (Fig. 3). One Mg²⁺ is located between His351 and Cys353 as
6 described in the ligand-free structure. The other Mg²⁺ is chelated by the β-carboxyl O atom
7 and the β-hydroxyl O atom of D-EHA, forming a D-EHA-Mg²⁺ complex. Thus, the latter Mg²⁺
8 is most likely accompanied by the presence of a ligand containing a β-carboxyl and
9 β-hydroxyl group. Electron density allowed the modeling of a covalent linkage between the
10 C4A atom of PLP and the α-amino group of D-EHA, generating an external aldimine bond.
11 The internal aldimine linkage between the cofactor and Lys43 appeared to be broken in the
12 electron density (Fig. S2b). Although significant structural differences were not observed, an
13 approximately 16° rotation of the cofactor pyridine ring was seen accompanied by the
14 Schiff-base interchange. The α-carboxyl group of D-EHA forms hydrogen bonds to the
15 guanidine group of Arg141 from the PLP-binding subunit and the main-chain N atom of
16 Gln319 from the neighbouring subunit. Note that the β-hydroxyl O atom of D-EHA is located
17 at a distance of 5.5 Å from the Mg²⁺ positioned between His351 and Cys353.
18 Crystallographic studies of chDSD have demonstrated that the Zn²⁺ sandwiched by His347
19 and Cys349 probably comes in contact with the β-hydroxyl group of D-serine and may have a
20 catalytic role in leaving the hydroxyl as a water molecule (Tanaka et al. 2011). Therefore, the
21 spatial arrangement of the hydroxyl group that lies far from the enzyme-coordinated Mg²⁺
22 presumably results in loss of the dehydration activity against D-EHA.

23

24 **Insights into the substrate binding**

25 To elucidate the structural mechanism of the substrate recognition of D-THA DH, we
26 have attempted to determine the structure of inactive mutant in complex with its substrate. We

1 generated the H351A and C353A mutants of D-THA DH and performed an enzyme assay
2 using D-THA and L-EHA as substrates. The results demonstrated that both H351A and C353A
3 mutations significantly decrease the activity towards D-THA and L-EHA (Table 2), similar to
4 the results obtained with scDSD (Ito et al. 2012). In particular, the specific activity of C353A
5 mutant towards D-THA and L-EHA was below the detection limit, indicating that Cys353 is a
6 key determinant of the enzymatic activity of D-THA DH. We have first determined the crystal
7 structures of H351A and C353A in the substrate-free form at resolutions of 1.7 and 1.55 Å,
8 respectively. Crystals of each mutant were obtained under the same crystallization condition
9 as for the wild-type D-THA DH. In the structure of the H351A mutant, Mg²⁺ occupies a
10 position near the side chain of Cys353. It is coordinated in an octahedral geometry by the
11 thiol S atom of Cys353 and five water molecules, positioned from the metal center at
12 distances of about 3.6 and 2.0-2.1 Å, respectively. These observations indicate that the H351A
13 mutant utilizes only one cysteine residue for the metal binding. In contrast, no electron
14 density for a metal bound to the active-site pocket was observed in the structure of C353A
15 mutant. It is thus suggested that the Mg²⁺ is held by the side chain of Cys353 rather than by
16 that of His351. Even in the absence of the metal, the structure of C353A mutant displays a
17 conformation similar to the wild-type enzyme. It should also be noted that the short soak of
18 wild-type D-THA DH crystal into the metal-free solution led to the elimination of Mg²⁺ from
19 the active site (Table 1; PDB code, 3WQF). These suggest a low binding affinity of Mg²⁺, and
20 that the Mg²⁺ is not required for the structural stabilization of the enzyme.

21 Structures of the H351A co-crystallized with D-THA and L-EHA were also determined
22 at resolutions of 1.8 and 1.9 Å, respectively. The covalent linkages appear to be formed
23 between the PLP cofactor and the α -amino groups of substrates from the electron density map.
24 Attempts to solve the crystal structures of the C353A in complex with D-THA and L-EHA
25 were not successful. Mg²⁺ could not bind to the active site of C353A mutant, leading to a
26 significant decrease in its substrate binding affinity. The electron density map of the structure

1 of H351A co-crystallized with D-THA unexpectedly showed that the N-C^α-C^β-C^γ of a bound
2 substrate is roughly coplanar with the lacking β-hydroxyl group. This prompted us to build a
3 model of 2-amino maleic acid (Fig. 4, a and b). 2-Amino maleic acid is a likely product of the
4 dehydration of D-THA, and thus the current complex structure represents its intermediate state
5 in the catalytic cycle of D-THA DH (Fig. 5). The water molecule (Wat709A/Wat712B) located
6 near the intermediate C^β atom at a distance of 2.0 Å was probably generated by the
7 dehydratase reaction catalyzed by the H351A mutant. Water also interacts with the liberated
8 ε-amino group of Lys43 (2.9 Å), the phosphate group of PLP (2.5 Å) and the
9 cysteine-coordinated Mg²⁺ (2.3 Å). These observations indicate that the C^β-OH orientation of
10 D-THA would be an important factor contributing to the substrate recognition of D-THA DH.
11 In addition, Mg²⁺ might directly interact with the β-hydroxyl group of D-THA to promote the
12 dehydration reaction. Not only D-THA but also L-EHA is a good substrate for D-THA DH
13 (Maeda et al. 2010). In the structure of H351A co-crystallized with L-EHA, the electron
14 density corresponding to L-EHA was clearly visible (Fig. 4, c and d). The hydroxyl O atom of
15 L-EHA occupies roughly the same position as Wat709A/Wat712B liberated from D-THA in
16 the reaction intermediate complex, and is also in direct contact with the Mg²⁺. Thus, the
17 substrate stereospecificity of D-THA DH is determined by the C^β-OH orientation of the
18 substrate at the active site.

19 In summary, we have determined three complex structures that shed light on the
20 3-hydroxyaspartate-recognition mechanism of D-THA DH: the wild-type enzyme in complex
21 with D-EHA, the H351A mutant in complex with 2-amino maleic acid originating from
22 D-THA, and the H351A mutant in complex with L-EHA. Obtaining the complex structure
23 with L-THA was tried with both the wild-type and the H351A mutant enzymes, however,
24 there was no visible electron density for L-THA in the active-site pockets. This was explained
25 by the high K_m value of D-THA DH for L-THA (K_m = 6.16 mM; Maeda et al. 2010).
26 Interestingly, the current structural studies revealed that chirality at the C^β position of

1 3-hydroxyaspartate (3*R*) can be well recognized by D-THA DH as substrates. The C^β
2 configuration of D-THA superimposed well onto that of L-EHA in the present models, which
3 is associated with the high levels of activities against D-THA and L-EHA. Thus, the active-site
4 conformation of D-THA DH would be compatible with the 3*R* configuration of
5 3-hydroxyaspartate. This finding provides an explanation for the efficient production of
6 optically pure 3-hydroxyaspartate having the 3*S* configuration as described below.

7

8 **Biocatalytic preparation of L-THA from DL-THA using D-THA DH**

9 We have developed a novel method for producing optically pure L-THA, which is
10 (2*S*,3*S*) form of 3-hydroxyaspartate and a promising intermediate for the synthesis of
11 L-TBOA, an important compound in understanding the regulatory functions of glutamate
12 transporters in the human brain (Shimamoto 2008). Enzyme kinetics and the structural
13 analysis have indicated that D-THA DH is useful in the dehydratase-catalyzed optical
14 resolution of DL-THA. Therefore, we evaluated the biocatalytic preparation of optically pure
15 L-THA by using purified D-THA DH. After 6 h, the enantiomeric excess (*e.e.*) of L-THA in
16 the reaction mixture reached >99% as calculated from the peak areas in the HPLC analysis
17 (Fig. 6a). In addition, the total concentration of DL-THA determined with an amino-acid
18 analyzer decreased to about half the initial value at the same time (Fig. S4). These results
19 indicate that D-THA in the racemate solution was enantioselectively converted to oxaloacetate
20 and ammonia by the enzymatic reaction. Remaining L-THA in the reaction product was
21 crystallized under the acidified condition (pH 2.0). The resulting residue was an enantiopure
22 L-THA as determined by HPLC analysis (Fig. S5). The isolation yield as dry weight was
23 38.9% against the amount of DL-THA initially added to the reaction mixture. Moreover,
24 chemical purity of the final product was verified by NMR analysis and it showed the
25 following signals (Fig. S6); ¹H NMR (500 MHz, TSP = 0 ppm): 3.98 (1H, d, *J* = 1.8 Hz), 4.52
26 (1H, d, *J* = 1.8 Hz) ppm; ¹³C NMR (125 MHz, TSP = 0 ppm): 60.02, 74.08, 176.47, 179.77

1 ppm. These signals indicate the *threo* isomer of 3-hydroxyaspartate.

2

3 **Biocatalytic preparation of D-EHA from DL-EHA by D-THA DH**

4 Similarly, biocatalytic preparation of optically pure D-EHA, which is
5 (2*R*,3*S*)-3-hydroxyaspartate, from DL-EHA was achieved by using purified D-THA DH. The
6 derivative of D-EHA, D-*erythro*- β -benzyloxyaspartate (D-EBOA) was also found to act as a
7 blocker for EAATs although the effect was relatively weak (Shimamoto et al., 2000). After 10
8 h of bioconversion, the reaction mixture contained only the D-enantiomer of
9 *erythro*-3-hydroxyaspartate with >99% *e.e.* and 48.9% of the isolated yield (Fig. 6b; Fig. S7).
10 The result of NMR signals verified the chemical purity of the final product as *erythro* isomer
11 of 3-hydroxyaspartate (Fig. S8); ¹H NMR (500 MHz, TSP = 0 ppm): 4.00 (1H, d, *J* = 3.6 Hz),
12 4.33 (1H, d, *J* = 3.6 Hz) ppm; ¹³C NMR (125 MHz, TSP = 0 ppm): 60.86, 74.47, 175.12,
13 179.16 ppm.

14

15

1 **Discussion**

2

3 **Structure comparison with D-serine dehydratase from chicken kidney**

4 Pairwise structure comparison using the *DALI* server (Holm and Park 2000) showed
5 that D-THA DH is structurally homologous to D-serine dehydratase from chicken kidney
6 (chDSD; Tanaka et al. 2011; PDB code, 3ANU; Z score, 45.2; rmsd, 1.9 Å for 358 C^α atoms;
7 sequence identity for fit regions, 37%). Although the overall fold of D-THA DH and chDSD
8 are identical, there are apparent differences that need to be discussed. The first difference is
9 the oligomerization state in the solution. Tanaka et al. based on the gel-filtration
10 chromatography results have reported that chDSD forms a dimer in the solution. Even though
11 crystallographic studies of chDSD demonstrate that the asymmetric unit comprises of a single
12 monomer, the biological assembly is assumed head-to-tail dimer. It is created by a
13 crystallographic 2-fold axis involving large and hydrophilic interface between the subunits. In
14 contrast to chDSD, judging from its apparent molecular mass analyzed by the gel filtration,
15 D-THA DH is a monomeric enzyme as previously reported (Maeda et al. 2010). However, as
16 shown in the present study, all the crystal forms of D-THA DH have the head-to-tail dimer in
17 the asymmetric unit, similar to the biological assembly of chDSD. The dimeric state of
18 D-THA DH revealed that the amino-acid residues Asn318-His321, which form a loop in the
19 C-terminal domain, contact neighboring PLP-binding pockets and include a Gln319 that is
20 expected to be utilized for D-EHA, D-THA and L-EHA binding. Each domain is also
21 responsible for the dimerization through hydrogen bonds. Therefore, the current symmetric
22 dimer is likely to be one of the possible conformational states of D-THA DH and the crystal
23 lattice forces may stabilize this conformation. The second difference is found in the
24 arrangement of residues that directly interact with the pyridine nitrogen, designated as N1.
25 The structure of chDSD revealed that the side chain of Tyr174 is within hydrogen-bonding
26 distance of N1. This environment may preclude the protonation of N1 that possibly functions

1 as a driving force for the catalysis of transamination. Therefore, the N1-unprotonated state of
2 chDSD is needed for the catalysis of β -elimination and for avoiding other PLP-catalyzed
3 reactions. Likewise, although the Tyr residue is substituted with Leu170 in D-THA DH based
4 on the primary structure alignment, the alternate Arg residue at position 234 is hydrogen
5 bonded to N1, thereby preventing proton transfer to N1 due to the high pK_a value of the
6 arginine side-chain (~ 12.5 in water).

7 In this structural study, Mg^{2+} was observed between the side chains of His351 and
8 Cys353, probably due to artificial crystallization solution containing 200 mM $MgCl_2$.
9 Although it is uncommon that Mg^{2+} is coordinated by imidazole and thiol ligands, the atomic
10 coordinates and the B-factor values were reasonably refined without extra F_o-F_c density map,
11 indicating that the bound metal is conclusively Mg^{2+} . The Mg^{2+} -free structure (Table 1; PDB
12 code, 3WQF) also suggests that D-THA DH has a low affinity for Mg^{2+} . To examine which
13 metals occupy the active site prior to crystallization, an inductively coupled plasma mass
14 spectrometry (ICP-MS) analysis was conducted on purified D-THA DH. The results showed
15 that a large amount of Zn^{2+} was detected in the purified enzyme (Fig. S9). A relatively high
16 content of Ni^{2+} and Co^{2+} was also detected after Ni^{2+} - and Co^{2+} -affinity purification,
17 respectively. Therefore, it can be concluded that D-THA DH naturally contains Zn^{2+} , but
18 under the given experimental conditions, the substitution of Zn^{2+} for other metals takes place
19 easily. Tanaka and co-workers have reported that chDSD naturally possesses Zn^{2+} based on its
20 X-ray structure, and only Mn^{2+} can partially substitute Zn^{2+} for the catalytic activity against
21 D-serine. In contrast, we have previously reported that D-THA DH works with a various
22 divalent cations such as Co^{2+} , Mn^{2+} , Ni^{2+} , Ca^{2+} , Zn^{2+} , and Fe^{2+} (Maeda et al. 2010).
23 Furthermore, addition of $MgCl_2$ to the enzyme solution after treatment with
24 ethylenediaminetetraacetic acid (EDTA) gave a low but significant recovery of the specific
25 activity of D-THA DH from 0.1 to 1.2 $\mu\text{mol}/\text{min}/\text{mg}$ protein (Fig. S3). This clearly shows that
26 the Mg^{2+} is functional and is involved in the enzymatic activity.

1
2
3
4
5
6
7
8
9
10
11
12
13
14
15
16
17
18
19
20
21
22
23
24
25
26

Insights into the catalytic mechanism and the substrate stereoselectivity

Note that the substitution of alanine for Cys353 precludes the binding of Mg^{2+} to D-THA DH (Table 1; PDB code, 3WQC). Structure of C353A mutant also showed no binding affinity towards D-EHA, D-THA and L-EHA (data not shown). Considering these results, it can be concluded that the substrate/inhibitor binding affinities of D-THA DH are greatly decreased by the absence of the metal. In contrast, crystallographic analysis have revealed that the pretreatment of EDTA allows chDSD to bind with D-serine even in the absence of Zn^{2+} . This suggests that chDSD does not require metal for the initial occurrence of the Schiff-base interchange from lysine-PLP to PLP-substrate.

On the basis of the X-ray structure of H351A cocrystallized with D-THA/L-EHA, a possible mechanism for the catalytic reaction of D-THA DH has been proposed (Fig. 5). Initially, the substrate covalently binds to the PLP molecule in each active-site pocket of the dimeric state of D-THA DH. Metal ion is also in direct contact with the β -carboxyl and β -hydroxyl O atoms, presumably playing a role in the stabilization of the bound substrate during the catalytic reaction. Upon abstracting a proton from the α -carbon of D-THA by Lys43 to generate a quinonoid resonance structure, the β -elimination reaction occurs by a proton donation to the substrate hydroxyl group. In previous structural studies on chDSD, the reported distance between the NZ atom of the Lys45 and the β -hydroxyl of D-serine was an optimal distance (3.2 Å) for the proton donation, suggesting that the abstracted α -proton could be transferred to the substrate hydroxyl *via* the lysine residue as an acid/base catalyst (Tanaka et al. 2011). In contrast, the current complex structures of the H351A mutant indicate that another candidate, a phosphate group of PLP, is located in the proper position contributing to the β -elimination reaction. We can assume that the protonated phosphate O atom acts as a general acid to donate a proton to the leaving hydroxyl group of the substrate. Indeed, the side chain of Tyr177 is in contact with the phosphate O atom, thus maintaining the protonation

1 state in transferring proton throughout the reaction. Also, the distances from the hydroxyl
2 group of substrate L-EHA to the ϵ -amino group of Lys43 (2.8 Å) and the phosphate group of
3 PLP (2.6 Å) are shorter than the corresponding distances from the hydroxyl group of inhibitor
4 D-EHA to the ϵ -amino group (5.8 Å) and the phosphate (5.7 Å). Considering that the ϵ -amino
5 group of Lys43 exhibits conformational dynamics in response to the catalytic cycle, the
6 association between the protonated phosphate group and the substrate hydroxyl is more
7 responsible for leaving the hydroxyl group as a water molecule. We observed the
8 PLP-2-amino maleic acid complex as the subsequent intermediate. An imine/enamine
9 released after the internal Schiff-base regeneration is thought to be hydrolyzed
10 non-enzymatically. Thus, tautomeric change of free 2-amino maleic acid into 2-imino succinic
11 acid and subsequent hydrolysis eliminate ammonia from the imine to give oxaloacetate.

12 C^{α} -H deprotonation is commonly carried out by the ϵ -amino group of a lysine that is
13 liberated from the internal aldimine with PLP (Toney 2005). In this study, the ϵ -amino group
14 of Lys43 could access the α -proton of D-THA, while it could not interact with that of L-EHA.
15 Alternatively, side-chains of Arg141 and His172 are situated close to the α -proton of L-EHA
16 and would play a role in the proton abstraction. Our previous kinetic analysis based on the
17 $k_{\text{cat}}/K_{\text{m}}$ values indicates that D-THA DH has 2.6-fold higher binding affinity for L-EHA than
18 for D-THA, thereby acting more effectively on L-EHA (Maeda et al. 2010). Since the only
19 difference between D-THA and L-EHA is the chirality at the C^{α} position (Fig. 1), it is
20 suggested that the α -proton abstraction from L-EHA by Arg141 and/or His172 might increase
21 the dehydratase activity. This raises the possibility that D-THA DH possesses the epimerase
22 activity between D-THA and L-EHA. However, the HPLC chromatograms can preclude this
23 possibility.

24

25 **Synthesis of optically pure 3-hydroxyaspartate using D-THA DH**

26 In this study, we have developed a novel synthetic approach leading to L-THA and

1 D-EHA *via* the dehydratase-catalyzed optical resolution. The separation of L-THA from the
2 corresponding racemate, DL-THA, was achieved by converting D-THA into oxaloacetate
3 using recombinant D-THA DH. Additionally, L-EHA also serves as a good substrate; therefore,
4 D-THA DH was also used for the synthesis of D-EHA starting from DL-EHA. To date, there
5 have been no published studies on an enzymatic optical resolution of racemic
6 3-hydroxyaspartates, although convenient synthetic routes for DL-THA and DL-EHA starting
7 from (\pm)-*trans*-epoxysuccinic acid were established many years ago (Kaneko and Katsura
8 1963). Thus, our data confirm for the first time the utility of D-THA DH as a biocatalyst for
9 the resolution of DL-*threo/erythro*-3-hydroxyaspartate.

10 The racemic mixture contains both enantiomers in equal amounts, and thus the
11 maximum yield in an optical resolution is 50%. Considering this theoretical maximum, the
12 synthetic approaches are quite efficient as judged from the isolated yields of L-THA and
13 D-EHA. However, D-THA DH was found to possess a slight activity against L-THA (Maeda et
14 al. 2010), resulting in a lower yield of L-THA (38.9%) compared to D-EHA (48.9%). There is
15 a need for further studies to create the mutant enzyme showing no activity on L-THA. In
16 addition, the reaction time of L-EHA degradation was longer than expected. This is likely due
17 to inhibition of the dehydratase by binding of D-EHA, which is the remaining product. Thus, a
18 short reaction time requires use of the mutant enzyme capable of overcoming the inhibition,
19 which could be accomplished by the structure-based engineering of D-THA DH whose
20 structure in complex with D-EHA has been reported here.

21 We confirmed the final products as pure L-THA and D-EHA by analyzing them with
22 TLC, HPLC, and NMR spectroscopy. We were able to isolate pure compounds directly by
23 recrystallization of the reaction mixtures; utilizing the lower solubility of 3-hydroxyaspartate
24 in acidic water (pH 2.0) compared to oxaloacetate and ammonia. Therefore, this synthetic
25 approach has an advantage for obtaining pure products without any chromatographic
26 purification. It is efficient and friendly to the environment because of minimal or no use of

1 organic solvents.

2 Strieker et al. (2008) reported that a single mutant of asparagine oxygenase
3 ($\text{AsnO}_{\text{D241N}}$) from *Streptomyces coelicolor* catalyzes one-step hydroxylation of L-aspartate to
4 produce L-THA. The bioconversion represents one of the simplest strategies for preparing
5 L-THA from a low-cost material. However, it is important to note that 1.16 g of the isolated
6 yield of L-THA per 100 mL of the reaction mixture was achieved in this study, which is a
7 considerable amount compared to the production data of Strieker et al. (14.8 mg of the
8 isolated yield per 10 mL of the reaction mixture). Strieker and co-workers have also reported
9 that the conversion reaction was carried out under optimized conditions including a low
10 temperature of 16 °C most probably due to the reduced enzyme stability of $\text{AsnO}_{\text{D241N}}$. In
11 contrast, D-THA DH was found to be thermally stable up to 45 °C (Fig. S10), which would be
12 more acceptable for industrial-scale reactions demanding moderate to high-temperature
13 conditions.

14

15

1 **Acknowledgments**

2 Authors would like to thank Dr. Eri Fukushi and Mr. Yusuke Takata of the GC-MS &
3 NMR Laboratory (Research Faculty of Agriculture, Hokkaido University) for assistance with
4 the NMR spectral measurements. We are grateful to Dr. Toshihiro Watanabe (Research
5 Faculty of Agriculture, Hokkaido University) for conducting the ICP-MS analysis. Authors
6 also acknowledge the technical staff at Photon Factory (PF) for their kind support in the X-ray
7 diffraction experiments. This work was financially supported in part by a grant-in-aid from
8 the Institute for Fermentation, Osaka (IFO). Synchrotron radiation experiments were
9 conducted under the approval of 2012G576 at PF.

10

11

1 **References**

2

3 Antolini L, Bucciarelli M, Caselli E, Davoli P, Forni A, Moretti I, Prati F, Torre G (1997)
4 Stereoselective synthesis of *erythro* β -substituted aspartates. J Org Chem 62:8784-8789. doi:
5 10.1021/jo971285+

6

7 Arriza JL, Eliasof S, Kavanaugh MP, Amara SG (1997) Excitatory amino acid transporter 5, a
8 retinal glutamate transporter coupled to a chloride conductance. Proc Natl Acad Sci U S A
9 94:4155-4160.

10

11 Arriza JL, Fairman WA, Wadiche JI, Murdoch GH, Kavanaugh MP, Amara SG (1994)
12 Functional comparisons of three glutamate transporter subtypes cloned from human motor
13 cortex. J Neurosci 14:5559-5569.

14

15 Battye TGG, Kontogiannis L, Johnson O, Powell HR, Leslie AGW (2011) iMOSFLM: a new
16 graphical interface for diffraction-image processing with MOSFLM. Acta Crystallogr Sect D
17 Biol Crystallogr 67:271-281. doi: 10.1107/S0907444910048675

18

19 Bionda N, Cudic M, Barisic L, Stawikowski M, Stawikowska R, Binetti D, Cudic P (2012) A
20 practical synthesis of N^{α} -Fmoc protected *L-threo*- β -hydroxyaspartic acid derivatives for
21 coupling via α - or β -carboxylic group. Amino Acids 42:285-293. doi:
22 10.1007/s00726-010-0806-x

23

24 Cardillo G, Gentilucci L, Tolomelli A, Tomasini C (1999) A practical method for the synthesis
25 of β -amino α -hydroxy acids. Synthesis of enantiomerically pure hydroxyaspartic acid and
26 isoserine. Synlett 11:1727-1730. doi: 10.1055/s-1999-2927

1
2 DeLano WL (2002) PyMOL. <http://www.pymol.org/>. Accessed 19 December 2014
3
4 Deng J, Hamada Y, Shioiri T (1995) Total synthesis of Alterobactin A, a super siderophore
5 from an open-ocean bacterium. *J Am Chem Soc* 117:7824-7825. doi: 10.1021/ja00134a035
6
7 Eliot AC, Kirsch JF (2004) Pyridoxal phosphate enzymes: Mechanistic, structural, and
8 evolutionary considerations. *Annu Rev Biochem* 73:383-415. doi:
9 10.1146/annurev.biochem.73.011303.074021
10
11 Emsley P, Cowtan K (2004) Coot: model-building tools for molecular graphics. *Acta*
12 *Crystallogr Sect D Biol Crystallogr* 60:2126-2132. doi: 10.1107/S0907444904019158
13
14 Hara R, Kino K (2010) Industrial production of *threo*-3-hydroxy-L-aspartic acid using
15 *Escherichia coli* resting cells. *J Biotechnol* 150S:373. doi: 10.1016/j.jbiotec.2010.09.450
16
17 Holm L, Park J (2000) DaliLite workbench for protein structure comparison. *Bioinformatics*
18 16:566-567. doi: 10.1093/bioinformatics/16.6.566
19
20 Ito T, Hemmi H, Kataoka K, Mukai Y, Yoshimura T (2008) A novel zinc-dependent D-serine
21 dehydratase from *Saccharomyces cerevisiae*. *Biochem J* 409:399-406. doi:
22 10.1042/BJ20070642
23
24 Ito T, Koga K, Hemmi H, Yoshimura T (2012) Role of zinc ion for catalytic activity in
25 D-serine dehydratase from *Saccharomyces cerevisiae*. *FEBS J* 279:612-624. doi:
26 10.1111/j.1742-4658.2011.08451.x

1
2 Kaneko T, Katsura H (1963) The synthesis of four optical isomers of β -hydroxyaspartic acid.
3 Bull Chem Soc Jap 36:899-903. doi: 10.1246/bcsj.36.899
4
5 Khalaf JK, Datta A (2008) A concise, asymmetric synthesis of (2*R*,3*R*)-3-hydroxyaspartic acid.
6 Amino Acids 35:507-510. doi: 10.1007/s00726-007-0595-z
7
8 Liu JQ, Dairi T, Itoh N, Kataoka M, Shimizu S (2003) A novel enzyme, D-3-hydroxyaspartate
9 aldolase from *Paracoccus denitrificans* IFO 13301: purification, characterization, and gene
10 cloning. Appl Microbiol Biotechnol 62:53-60. doi: 10.1007/s00253-003-1238-2
11
12 Maeda T, Takeda Y, Murakami T, Yokota A, Wada M (2010) Purification, characterization and
13 amino acid sequence of a novel enzyme, D-*threo*-3-hydroxyaspartate dehydratase, from
14 *Delftia* sp. HT23. J Biochem 148:705-712. doi: 10.1093/jb/mvq106
15
16 Matsumoto Y, Yasutake Y, Takeda Y, Tamura T, Yokota A, Wada M (2013) Crystallization and
17 preliminary X-ray diffraction studies of D-*threo*-3-hydroxyaspartate dehydratase isolated from
18 *Delftia* sp. HT23. Acta Crystallogr Sect F Struct Biol Cryst Commun 69:1131-1134. doi:
19 10.1107/S1744309113023956
20
21 Murakami T, Maeda T, Yokota A, Wada M (2009) Gene cloning and expression of pyridoxal
22 5'-phosphate-dependent L-*threo*-3-hydroxyaspartate dehydratase from *Pseudomonas* sp. T62,
23 and characterization of the recombinant enzyme. J Biochem 145:661-668. doi:
24 10.1093/jb/mvp023
25
26 Murshudov GN, Skubák P, Lebedev AA, Pannu NS, Steiner RA, Nicholls RA, Winn MD,

1 Long F, Vagin AA (2011) REFMAC5 for the refinement of macromolecular crystal structures.
2 Acta Crystallogr Sect D Biol Crystallogr 67:355-367. doi: 10.1107/S0907444911001314
3
4 Nakashima N, Tamura T (2004a) A novel system for expressing recombinant proteins over a
5 wide temperature range from 4 to 35°C. Biotechnol Bioeng 86:136-148. doi:
6 10.1002/bit.20024
7
8 Nakashima N, Tamura T (2004b) Isolation and characterization of a rolling-circle-type
9 plasmid from *Rhodococcus erythropolis* and application of the plasmid to
10 multiple-recombinant-protein expression. Appl Environ Microbiol 70:5557-5568. doi:
11 10.1128/AEM.70.9.5557-5568.2004
12
13 Schneider G, Käck H, Lindqvist Y (2000) The manifold of vitamin B₆ dependent enzymes.
14 Structure 8:R1-R6. doi: 10.1016/S0969-2126(00)00085-X
15
16 Sheldrick GM (2007) A short history of SHELX. Acta Crystallogr Sect A Found Crystallogr
17 64:112-122. doi: 10.1107/S0108767307043930
18
19 Shigeri Y, Seal RP, Shimamoto K (2004) Molecular pharmacology of glutamate transporters,
20 EAATs and VGLUTs. Brain Res Rev 45:250-265. doi: 10.1016/j.brainresrev.2004.04.004
21
22 Shigeri Y, Shimamoto K, Yasuda-Kamatani Y, Seal RP, Yumoto N, Nakajima T, Amara SG
23 (2001) Effects of *threo*- β -hydroxyaspartate derivatives on excitatory amino acid transporters
24 (EAAT4 and EAAT5). J Neurochem 79:297-302. doi: 10.1046/j.1471-4159.2001.00588.x
25
26 Shimamoto K (2008) Glutamate transporter blockers for elucidation of the function of

1 excitatory neurotransmission systems. Chem Rec 8:182-199. doi: 10.1002/tcr.20145
2
3 Shimamoto K, Lebrun B, Yasuda-Kamatani Y, Sakaitani M, Shigeri Y, Yumoto N, Nakajima T
4 (1998) DL-*threo*- β -benzyloxyaspartate, a potent blocker of excitatory amino acid transporters.
5 Mol Pharmacol 53:195-201.
6
7 Shimamoto K, Sakai R, Takaoka K, Yumoto N, Nakajima T, Amara SG, Shigeri Y (2004)
8 Characterization of novel L-*threo*- β -benzyloxyaspartate derivatives, potent blockers of the
9 glutamate transporters. Mol Pharmacol 65:1008-1015. doi: 10.1124/mol.65.4.1008
10
11 Shimamoto K, Shigeri Y, Yasuda-Kamatani Y, Lebrun B, Yumoto N, Nakajima T (2000)
12 Syntheses of optically pure β -hydroxyaspartate derivatives as glutamate transporter blockers.
13 Bioorg Med Chem Lett 10:2407-2410. doi: 10.1016/S0960-894X(00)00487-X
14
15 Strieker M, Essen LO, Walsh CT, Marahiel MA (2008) Non-heme hydroxylase engineering
16 for simple enzymatic synthesis of L-*threo*-hydroxyaspartic acid. ChemBioChem 9:374-376.
17 doi: 10.1002/cbic.200700557
18
19 Tanaka H, Senda M, Venugopalan N, Yamamoto A, Senda T, Ishida T, Horiike K (2011)
20 Crystal structure of a zinc-dependent D-serine dehydratase from chicken kidney. J Biol Chem
21 286:27548-27558. doi: 10.1074/jbc.M110.201160
22
23 Tanaka H, Yamamoto A, Ishida T, Horiike K (2008) D-serine dehydratase from chicken
24 kidney: a vertebral homologue of the cryptic enzyme from *Burkholderia cepacia*. J Biochem
25 143:49-57. doi: 10.1093/jb/mvm203
26

1 Terwilliger TC (2000) Maximum-likelihood density modification. Acta Crystallogr Sect D
2 Biol Crystallogr 56:965-972.
3
4 Terwilliger TC, Berendzen J (1999) Automated MAD and MIR structure solution. Acta
5 Crystallogr Sect D Biol Crystallogr 55:849-861. doi: 10.1107/S09074444999000839
6
7 Toney MD (2005) Reaction specificity in pyridoxal phosphate enzymes. Arch Biochem
8 Biophys 433:279-287. doi: 10.1016/j.abb.2004.09.037
9
10 Wada M, Matsumoto T, Nakamori S, Sakamoto M, Kataoka M, Liu JQ, Itoh N, Yamada H,
11 Shimizu S (1999) Purification and characterization of a novel enzyme,
12 *L-threo*-3-hydroxyaspartate dehydratase, from *Pseudomonas* sp. T62. FEMS Microbiol Lett
13 179:147-151.
14
15 Wada M, Nakamori S, Takagi H (2003) Serine racemase homologue of *Saccharomyces*
16 *cerevisiae* has *L-threo*-3-hydroxyaspartate dehydratase activity. FEMS Microbiol Lett
17 225:189-193. doi: 10.1016/S0378-1097(03)00484-1
18
19 Winn MD, Ballard CC, Cowtan KD, Dodson EJ, Emsley P, Evans PR, Keegan RM, Krissinel
20 EB, Leslie AGW, McCoy A, McNicholas SJ, Murshudov GN, Pannu NS, Potterton EA,
21 Powell HR, Read RJ, Vagin A, Wilson KS (2011) Overview of the CCP4 suite and current
22 developments. Acta Crystallogr Sect D Biol Crystallogr 67:235-242. doi:
23 10.1107/S09074444910045749
24
25

1 **Figure Captions**

2

3 **Figure 1**

4 Structures of the four 3-hydroxyaspartate stereoisomers. L-THA,
5 *L-threo*-3-hydroxyaspartate; D-THA, *D-threo*-3-hydroxyaspartate; L-EHA,
6 *L-erythro*-3-hydroxyaspartate; D-EHA, *D-erythro*-3-hydroxyaspartate.

7

8 **Figure 2**

9 Structure of D-THA DH from *Delftia* sp. HT23 (a) Ribbon diagram of the dimeric
10 structure where one of the monomers is colored in green and the other in yellow. The PLP
11 cofactor is shown as a stick model colored in magenta, and the Mg²⁺ between side-chains of
12 His351 and Cys353 is shown as a sphere in blue. (b) Ribbon diagram of the monomeric
13 structure. The α -helices and β -strands, and loops are colored in red, yellow, and green,
14 respectively. The α -helices and β -strands are labeled numerically from the N- to C-terminus
15 (α 1- α 8 and β 1- β 17). (c) Stereo-view showing the cofactor-binding site of D-THA DH in the
16 substrate-free form. Side-chains interacting with PLP and Mg²⁺ are shown as sticks and
17 labeled. The surrounding polypeptide chain is represented as a semi-transparent ribbon
18 diagram colored in green.

19

20 **Figure 3**

21 Stereo-view of the active-site structure of D-THA DH with the bound inhibitor
22 (D-EHA). The functionally important residues (in green), PLP (in magenta), and bound
23 D-EHA (in yellow) are shown as sticks and labeled. Mg²⁺ is shown as blue spheres.

24

25 **Figure 4**

26 2-Amino maleic acid and L-EHA binding to the H351A mutant of D-THA DH. (a) An

1 mF_o-DF_c omit map for bound 2-amino maleic acid and the water molecule
2 (Wat709A/Wat712B) is shown. The map was contoured at the 2.8σ level. (b) Stereo-view
3 representation of the active-site structure of the H351A mutant with the reaction intermediate
4 2-amino maleic acid. The functionally important residues including mutational residue
5 Ala351 (in green), PLP (in magenta), and 2-amino maleic acid (in yellow) are shown as sticks
6 and labeled. The nearest water molecule (Wat709A/Wat712B) from the intermediate C^β atom
7 is also shown in red and Mg^{2+} in blue. (c) An mF_o-DF_c omit map for bound L-EHA is shown.
8 The map was contoured at 2.6σ level. (d) Stereo-view representation of the active-site
9 structure of the H351A mutant with substrate L-EHA. This image was prepared in the same
10 way and in the same orientation as that of panel *b*.

11

12 **Figure 5**

13 Proposed catalytic cycle of D-THA DH based on the structure of the H351A mutant in
14 complex with 2-amino maleic acid. Initial addition of the substrate converts lysine-PLP
15 (internal aldimine) to PLP-D-THA (external aldimine). Next, proton abstraction from the
16 α -carbon of bound D-THA occurs by Lys43 (Arg141 and/or His172 in the case of L-EHA) to
17 generate a quinonoid intermediate. The PLP-2-amino maleic acid complex is subsequently
18 generated by the β -elimination reaction promoted by the interaction between the hydroxyl O
19 atom and the active-site metal ion (represented as M^{2+}). The protonated phosphate of PLP acts
20 as an acid to donate its proton to the hydroxyl, which is then released as water. Finally,
21 regeneration of the internal aldimine linkage and non-enzymatic hydrolysis of the resulting
22 free imine/enamine release oxaloacetate and ammonia.

23

24 **Figure 6**

25 Optically pure production of L-THA and D-EHA. (a) Biocatalytic preparation of
26 L-THA from DL-THA by purified D-THA DH. The reaction mixture consisted of 100 mM

1 Tris-HCl buffer (pH 8.0), 0.01 mM PLP, 0.1 mM MnCl₂, 200 mM DL-THA, and 0.66 mg of
2 the enzyme in a total volume of 100 mL. During incubation, the D-form and L-form of
3 3-hydroxyaspartate in the reaction mixture were monitored using HPLC. The enantiomeric
4 excess (*e.e.*) was calculated from the peak areas of the stereoisomers. (b) Biocatalytic
5 preparation of D-EHA from DL-EHA by purified D-THA DH. The experiment and calculation
6 were performed with the same procedure as for the production of L-THA except for an
7 enzyme amount of 0.87 mg.
8

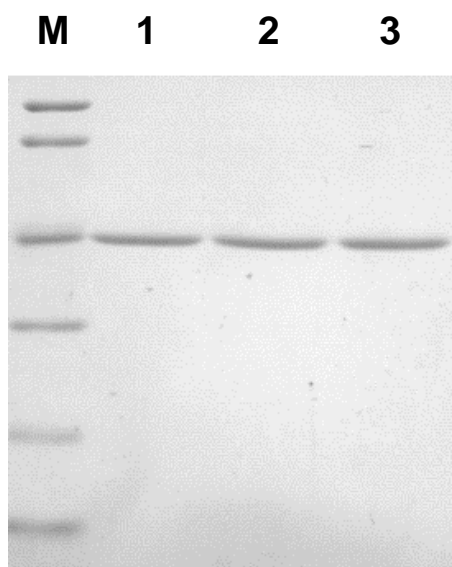


Figure S1 SDS-PAGE of the wild-type and mutants of D-THA DH. *Lanes 1-3* correspond to the wild-type, H351A, and C353A mutants, respectively. *Lane M* contains marker proteins, including (from *top* to *bottom*), phosphorylase (M_r , 97,400), bovine serum albumin (66,300), aldolase (42,400), carbonic anhydrase (30,000), trypsin inhibitor (20,100), and lysozyme (14,400). Gel was stained for protein with Coomassie Brilliant Blue R-250 (Wako Pure Chemical Industries).

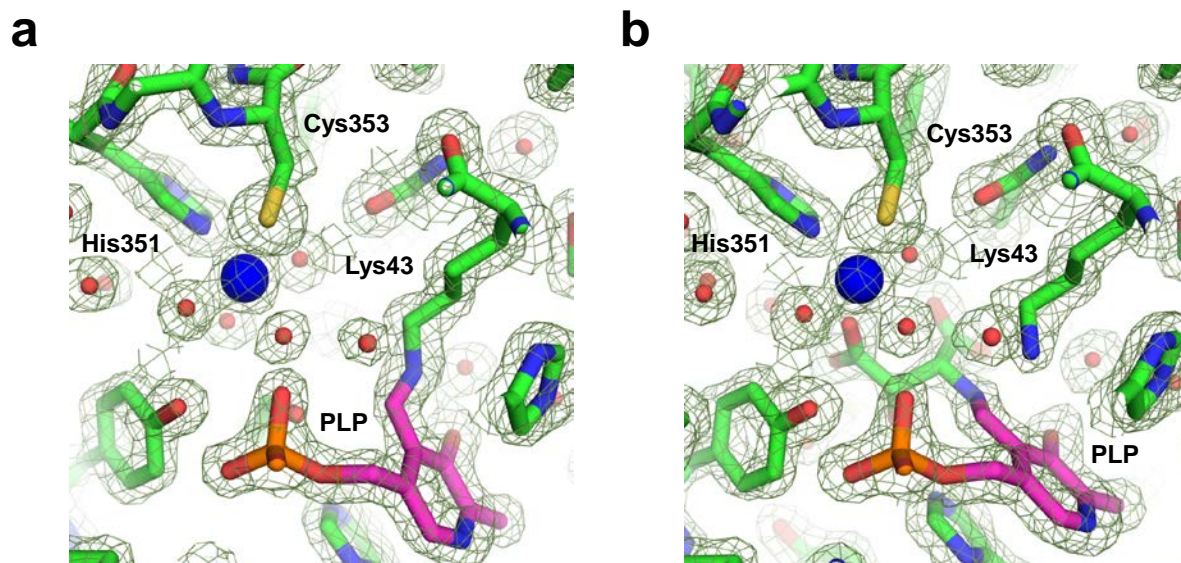


Figure S2 Final $2mF_o-DF_c$ map of the wild-type D-THA DH around active site in (a) substrate-free form (PDB code, 3WQC) and in (b) complex with D-EHA (PDB code, 3WQD), clearly showing the Schiff-base interchange from lysine-PLP to PLP-D-EHA. Each map was shows contours at 1.4σ level.

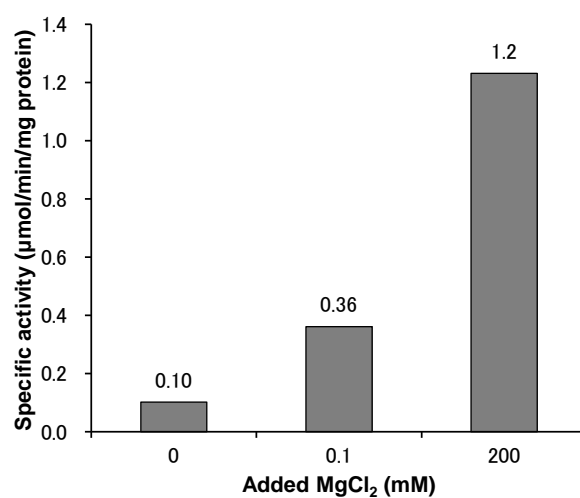


Figure S3 Effect of Mg²⁺ on the specific activity of D-THA DH. EDTA-treated enzyme was prepared using the method described earlier (Maeda et al. 2010). It was incubated for 10 min with the reaction mixture in the absence of any metal, or in the presence of 0.1 or 200 mM MgCl₂. The dehydratase activity was then measured. Addition of MgCl₂ increases the specific activity of the EDTA-treated D-THA DH.

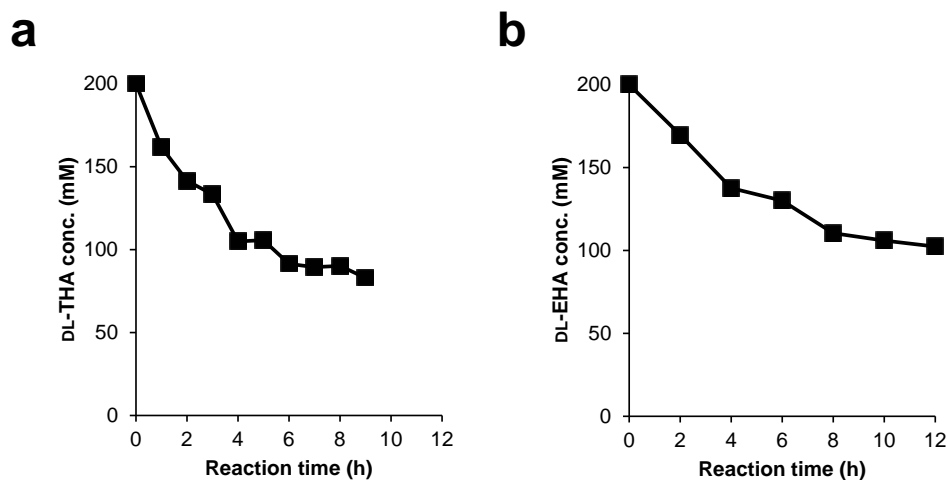


Figure S4 Time-dependent changes in the total concentration of (a) DL-THA and (b) DL-EHA in the reaction mixture. The concentration in the sample of 0 h incubation was taken as 200 mM, and the relative values for following samples were obtained. Total concentration of DL-THA and DL-EHA decreases to about half the initial value when the enantiomeric excess (*e.e.*) of L-THA and D-EHA in the reaction mixture reaches >99%, respectively.

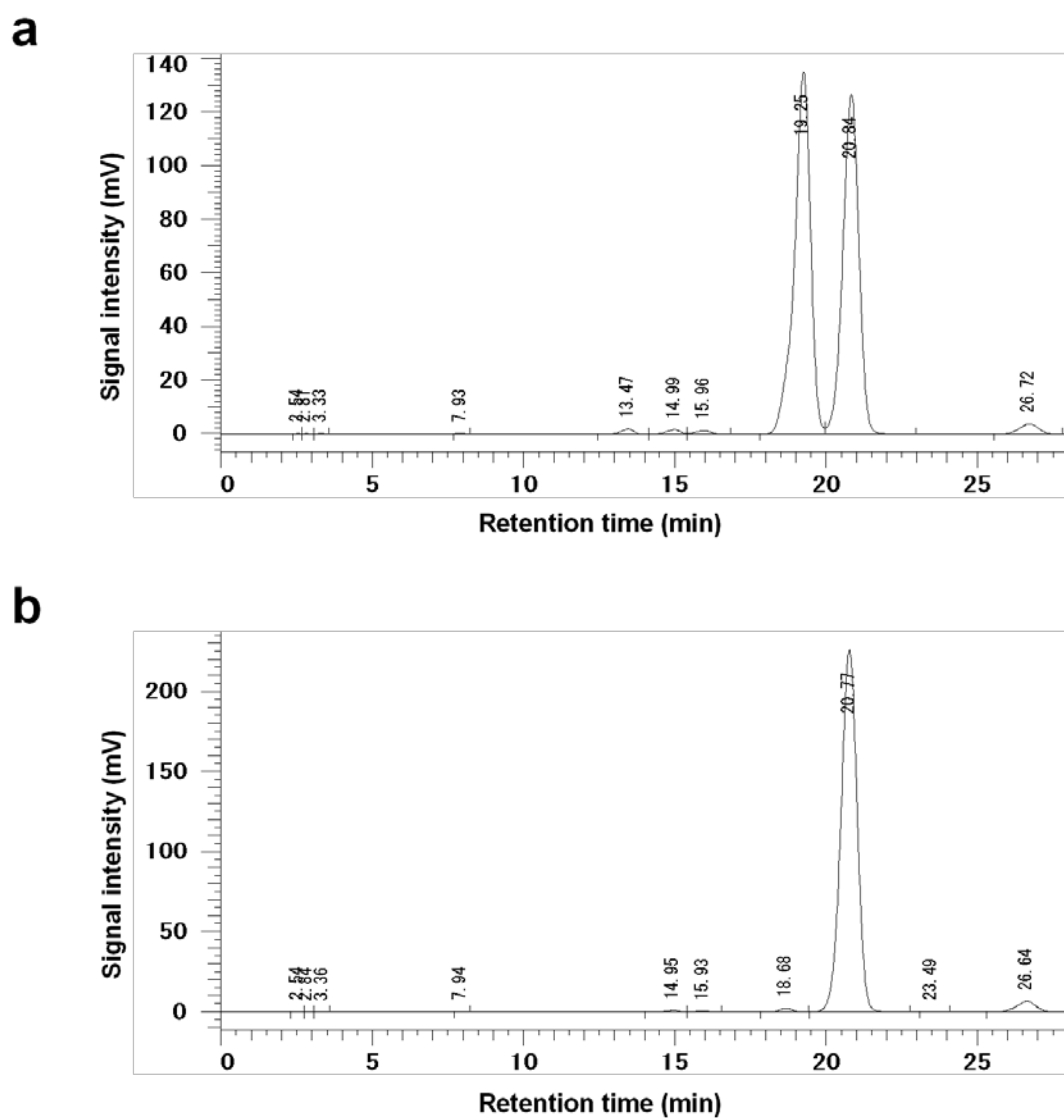
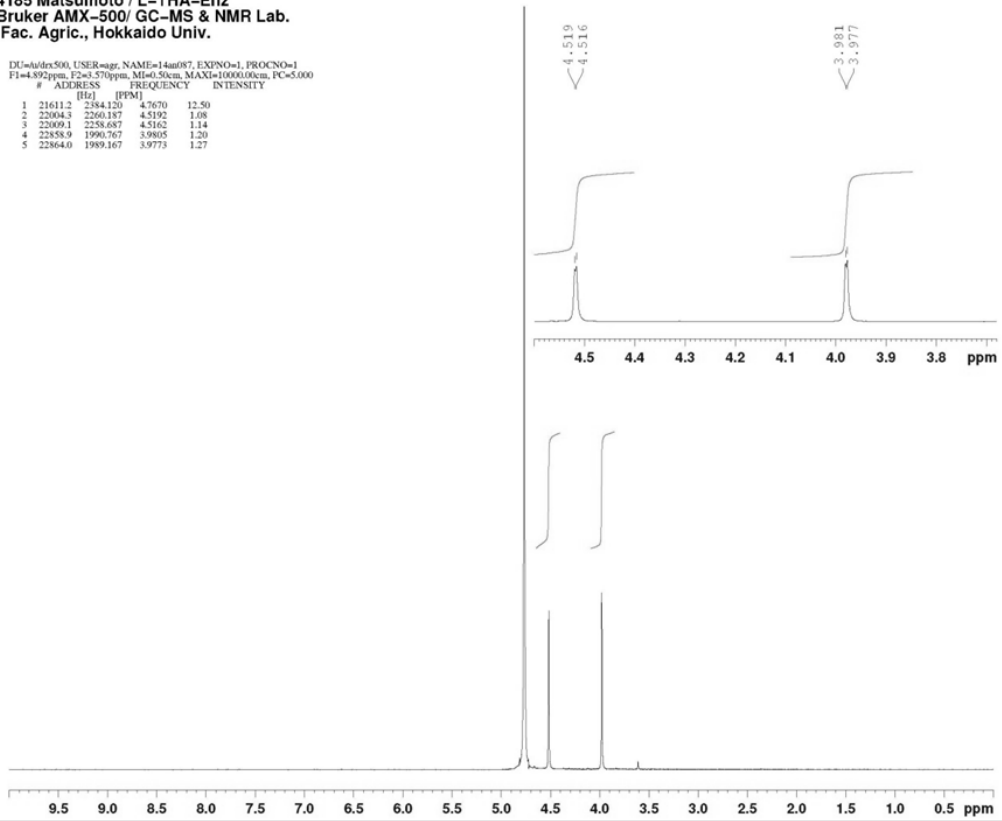


Figure S5 HPLC chromatograms recorded at 250 nm of (a) DL-THA purchased from Tokyo Chemical Industry and (b) L-THA obtained by enzymatic optical resolution. Samples were derivatized with GITC and the derivatives were analyzed using HPLC at a flow rate of 1.0 mL min⁻¹ with 30% methanol in water as the mobile phase. Retention times of the D/L-enantiomer of *threo*-3-hydroxyaspartate were 19.25/20.84 min.

a

4185 Matsumoto / L-THA-Enz
 Bruker AMX-500/ GC-MS & NMR Lab.
 Fac. Agric., Hokkaido Univ.

DU=sdex500, USER=aggr, NAME=14an087, EXPNO=1, PROCNO=1
 F1=4.892ppm, F2=3.570ppm, M1=0.50cm, MAX1=10000.00cm, PC=5.000
 # ADDRESS FREQUENCY INTENSITY
 [Hz] [PPM]
 1 21611.2 2384.120 4.7670 12.50
 2 22004.3 2260.187 4.5192 1.08
 3 22009.1 2258.687 4.5162 1.14
 4 22858.9 1990.767 3.9805 1.20
 5 22864.0 1989.167 3.9773 1.27

**b**

4185 Matsumoto / L-THA-Enz
 Bruker AMX-500/ GC-MS & NMR Lab.
 Fac. Agric., Hokkaido Univ.

DU=01, USER=aggr, NAME=14an087, EXPNO=2, PROCNO=1
 F1=232.138ppm, F2=-6.655ppm, M1=0.00cm, MAX1=13.00cm, PC=3.000
 # ADDRESS FREQUENCY INTENSITY
 [Hz] [PPM]
 1 7185.8 22607.265 179.7688 5.09
 2 7638.7 22192.152 176.4679 4.85
 3 21688.5 9316.350 74.0819 12.50
 4 23618.3 7847.786 60.0186 11.30

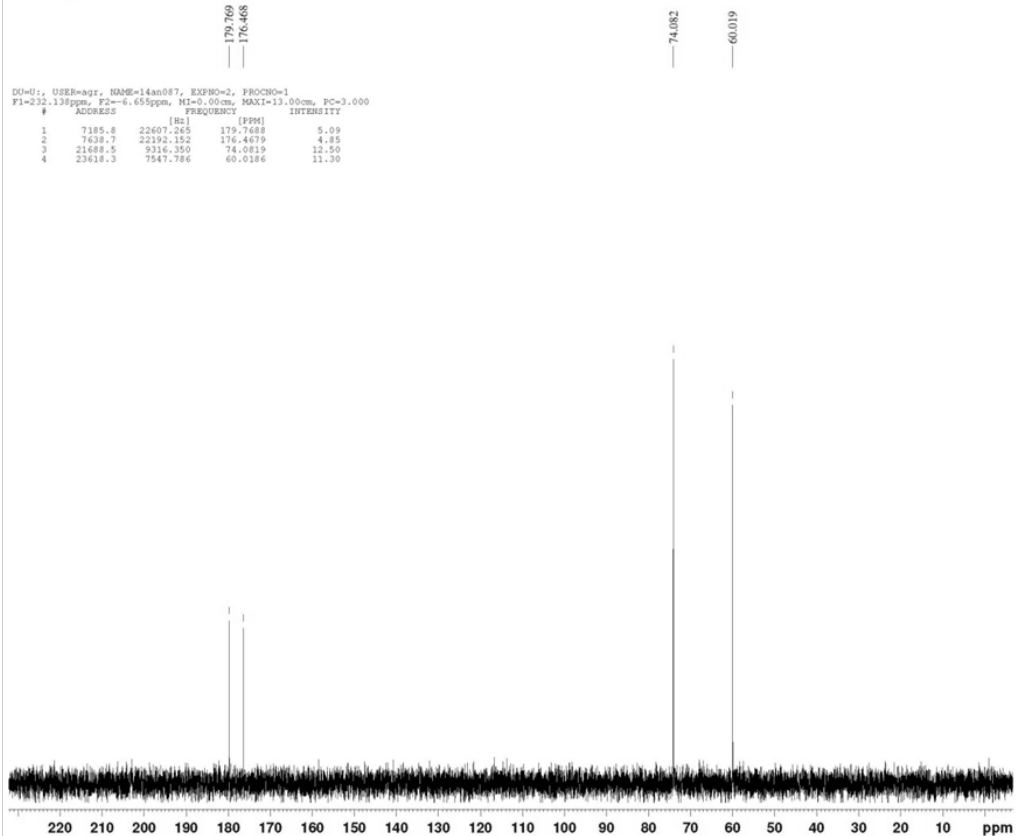


Figure S6 (a) ^1H NMR spectra recorded at 500 MHz and (b) ^{13}C NMR spectra recorded at 125 MHz of L-THA obtained by enzymatic optical resolution. Note that the ^1H signal at 4.77 ppm is attributed to deuterium oxide (D_2O).

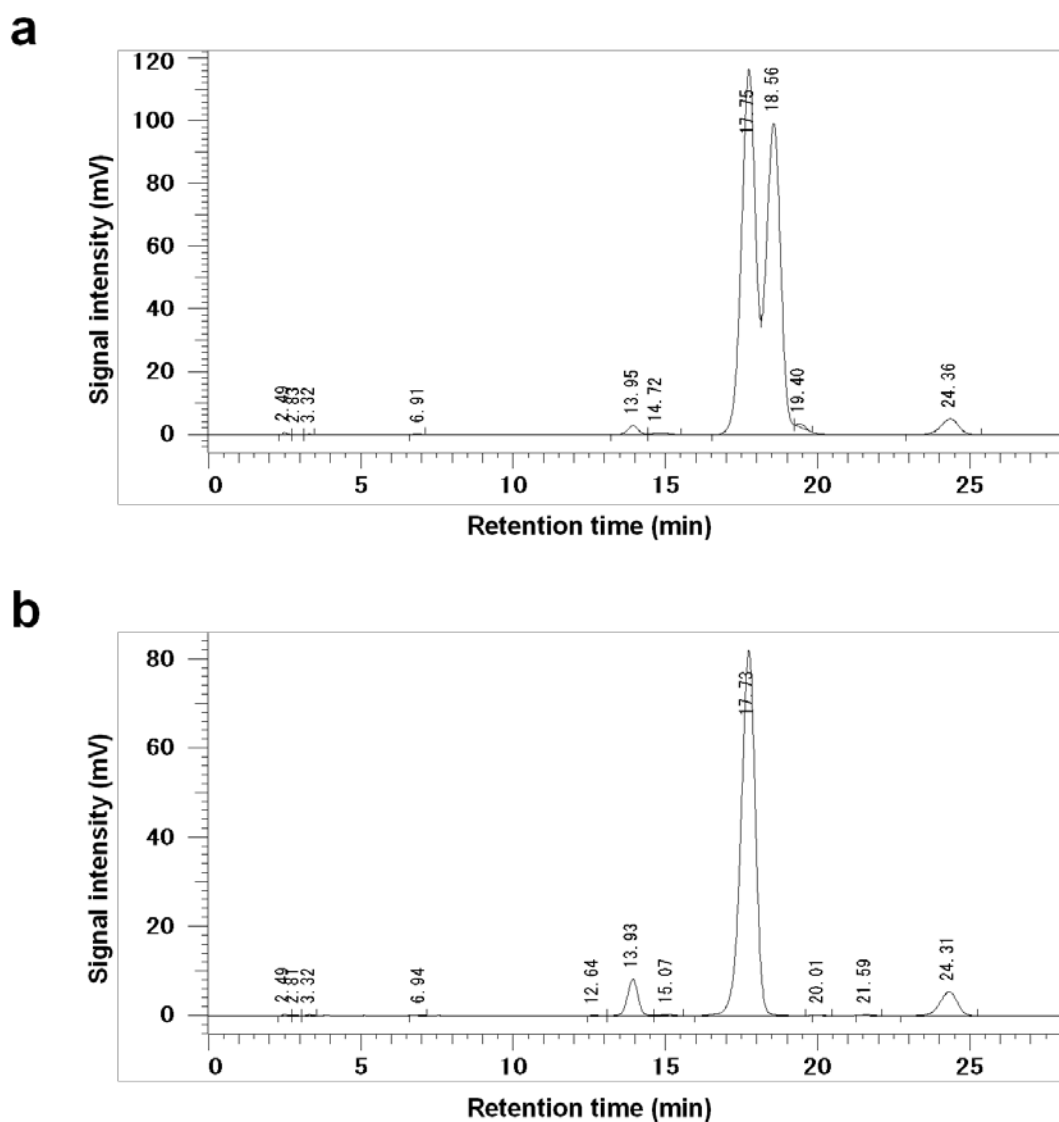
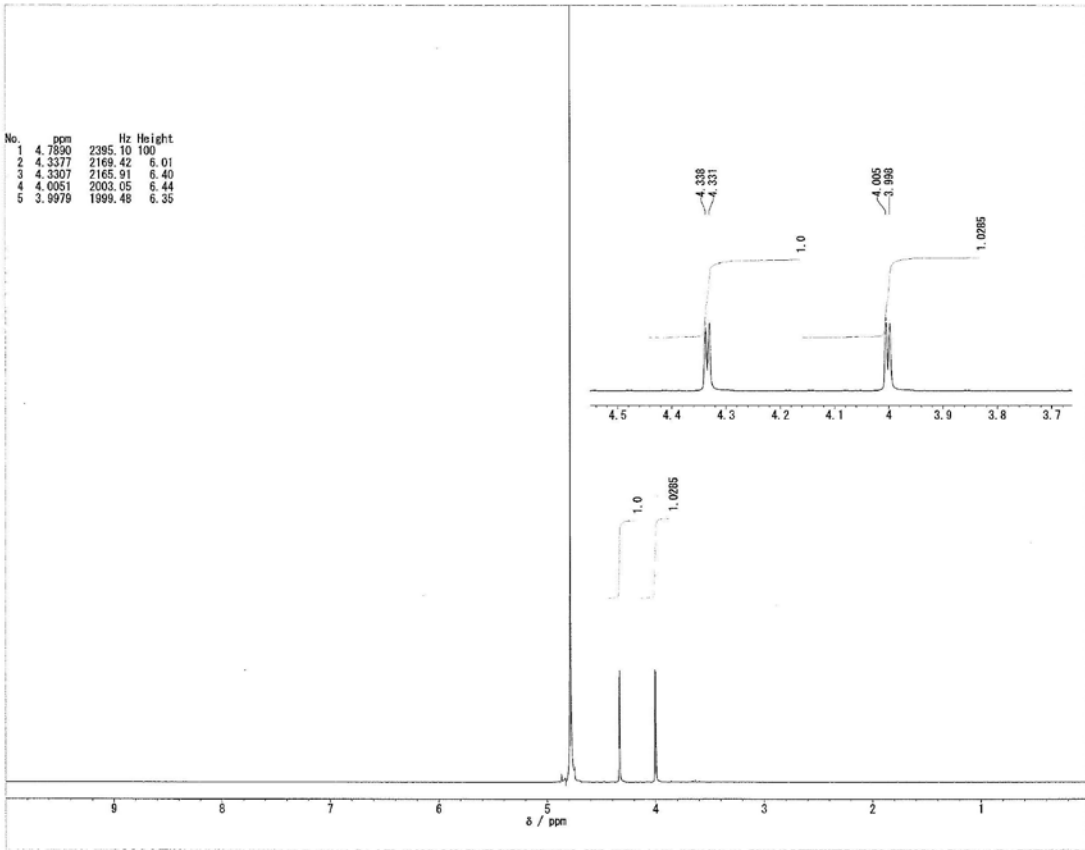


Figure S7 HPLC chromatograms recorded at 250 nm of (a) DL-EHA synthesized by the protocol described in the Materials and methods and (b) D-EHA obtained by enzymatic optical resolution. Samples were derivatized with GITC and the derivatives were analyzed using HPLC at a flow rate of 1.0 mL min^{-1} with 35% methanol in water as the mobile phase. Retention times of the D/L-enantiomer of *erythro*-3-hydroxyaspartate were 17.75/18.56 min.

a



b

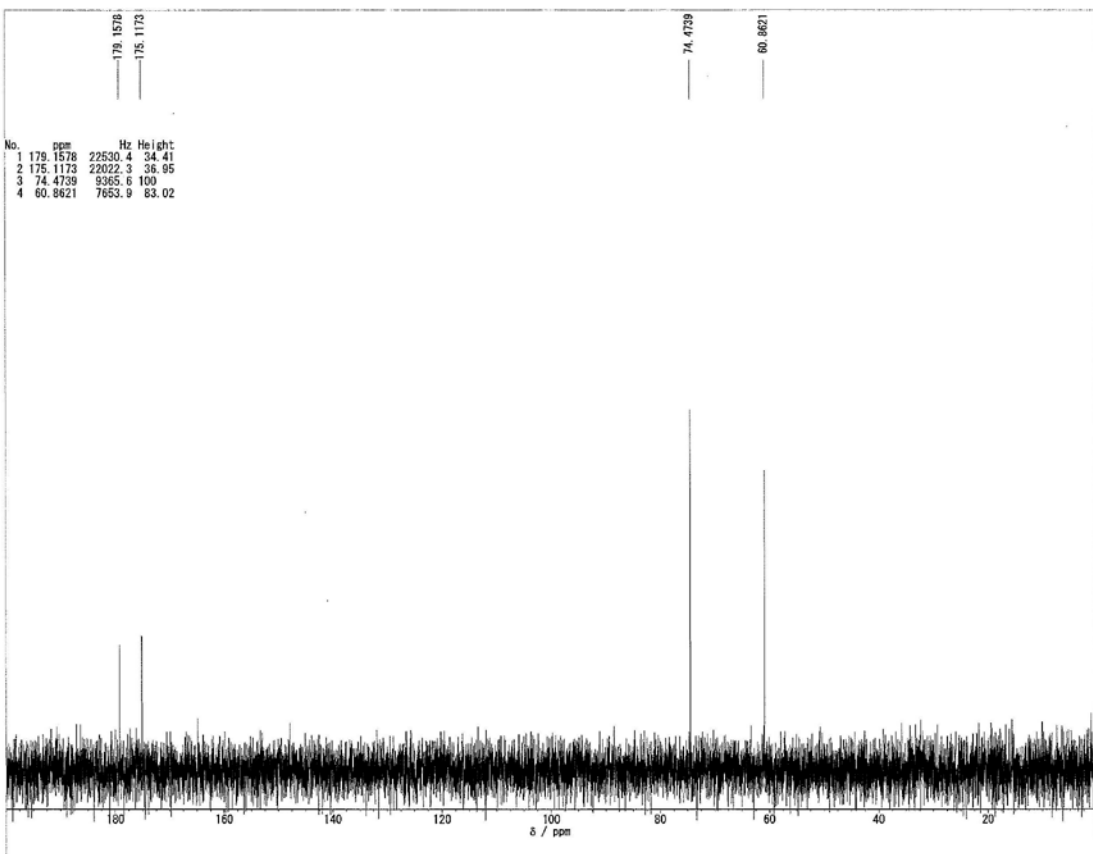


Figure S8 (a) ^1H NMR spectra recorded at 500 MHz and (b) ^{13}C NMR spectra recorded at 125 MHz of D-EHA obtained by enzymatic optical resolution. Note that the ^1H signal at 4.79 ppm is attributed to deuterium oxide (D_2O).

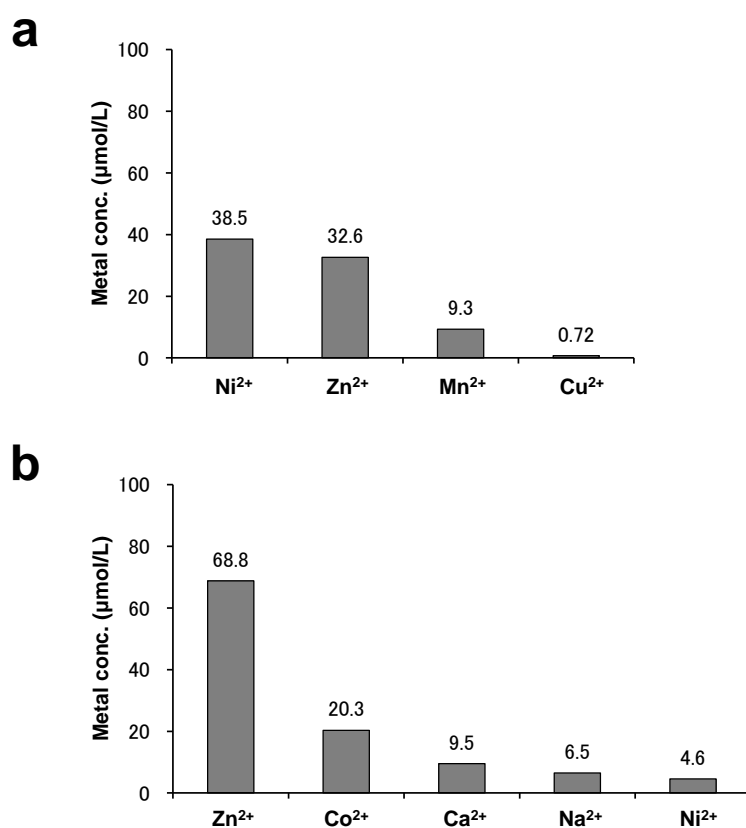


Figure S9 The metal concentration in the solution of recombinant D-THA DH purified by (a) HisTrap Ni²⁺-affinity column (GE Healthcare, Little Chalfont, UK) and (b) HisTALON Co²⁺-affinity column (Clontech Laboratories, Inc., Mountain View, CA). These were determined by inductively coupled plasma mass spectrometry (ICP-MS; ELAN DRC-e; Perkin Elmer, Waltham, MA). Enzyme concentrations were taken as 100 μmol/L. Shown are the five top-ranked metals for each analysis (Only four metals were detected in the sample of *a*). Large amount of Zn²⁺ was detected along with a relatively high content of Ni²⁺ and Co²⁺ after purification by Ni²⁺- and Co²⁺-affinity chromatography, respectively. There was a slight or no concentration of Mg²⁺.

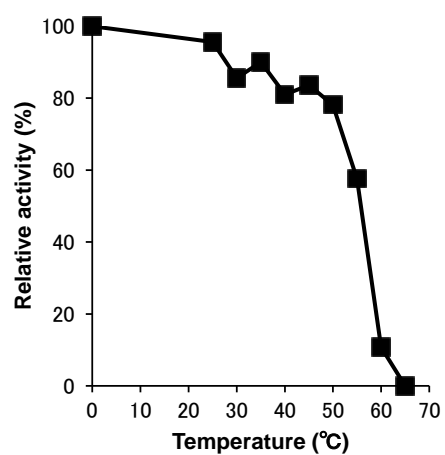
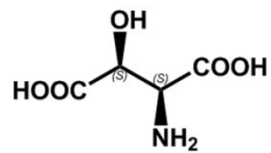
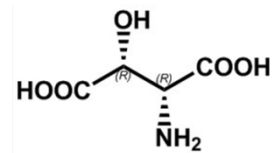


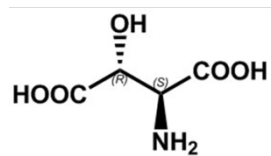
Figure S10 Thermal stability of D-THA DH. Purified D-THA DH solution was incubated for 15 min at different temperatures (0-65 °C). After incubation, it was placed on ice for 5 min and then the residual dehydratase activity was assayed by the protocol described in the Materials and methods. The activity of the enzyme incubated at 0 °C was taken as 100%. Over 80% of the residual activity was present in the range of temperature between 0 and 45 °C.



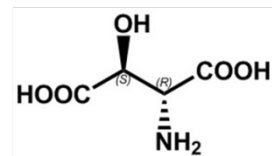
L-THA (2S,3S)



D-THA (2R,3R)



L-EHA (2S,3R)



D-EHA (2R,3S)

Fig. 1 Matsumoto et al.

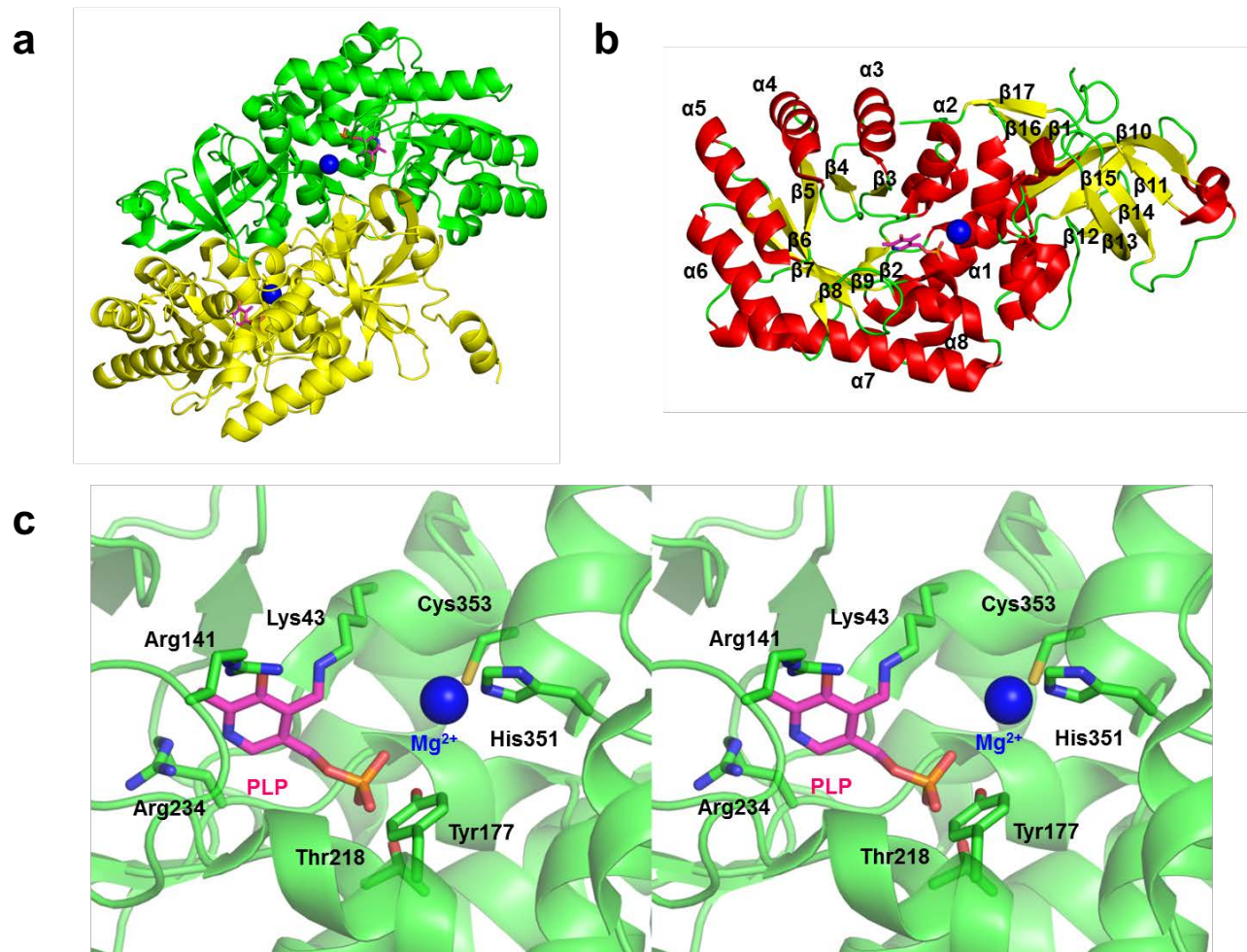


Fig. 2 Matsumoto et al.

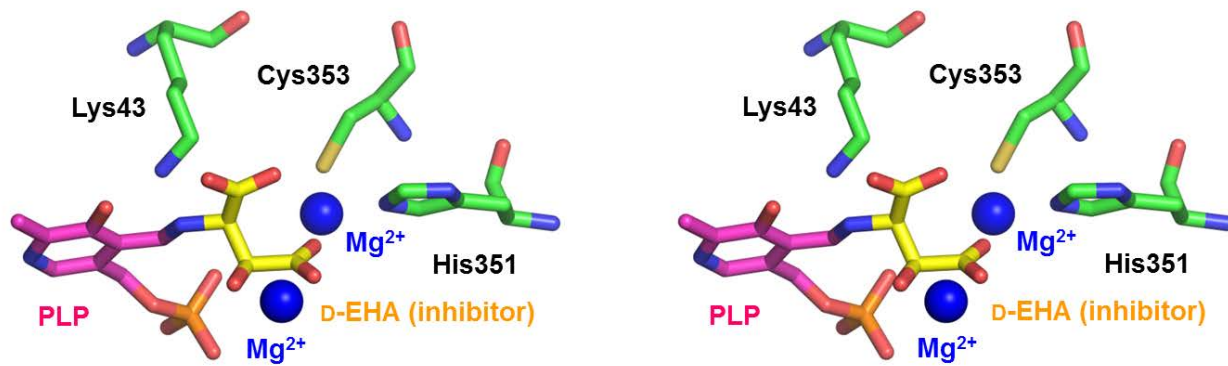


Fig. 3 Matsumoto et al.

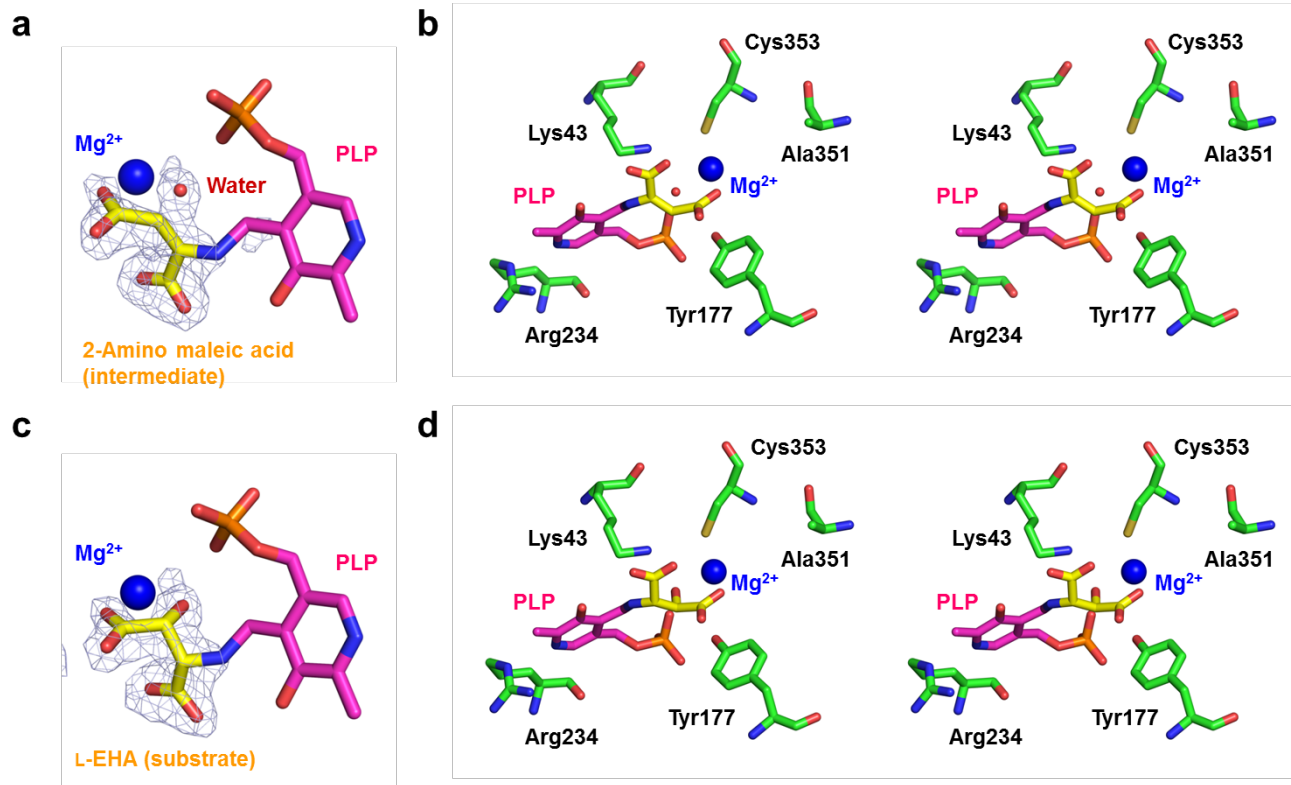


Fig. 4 Matsumoto et al.

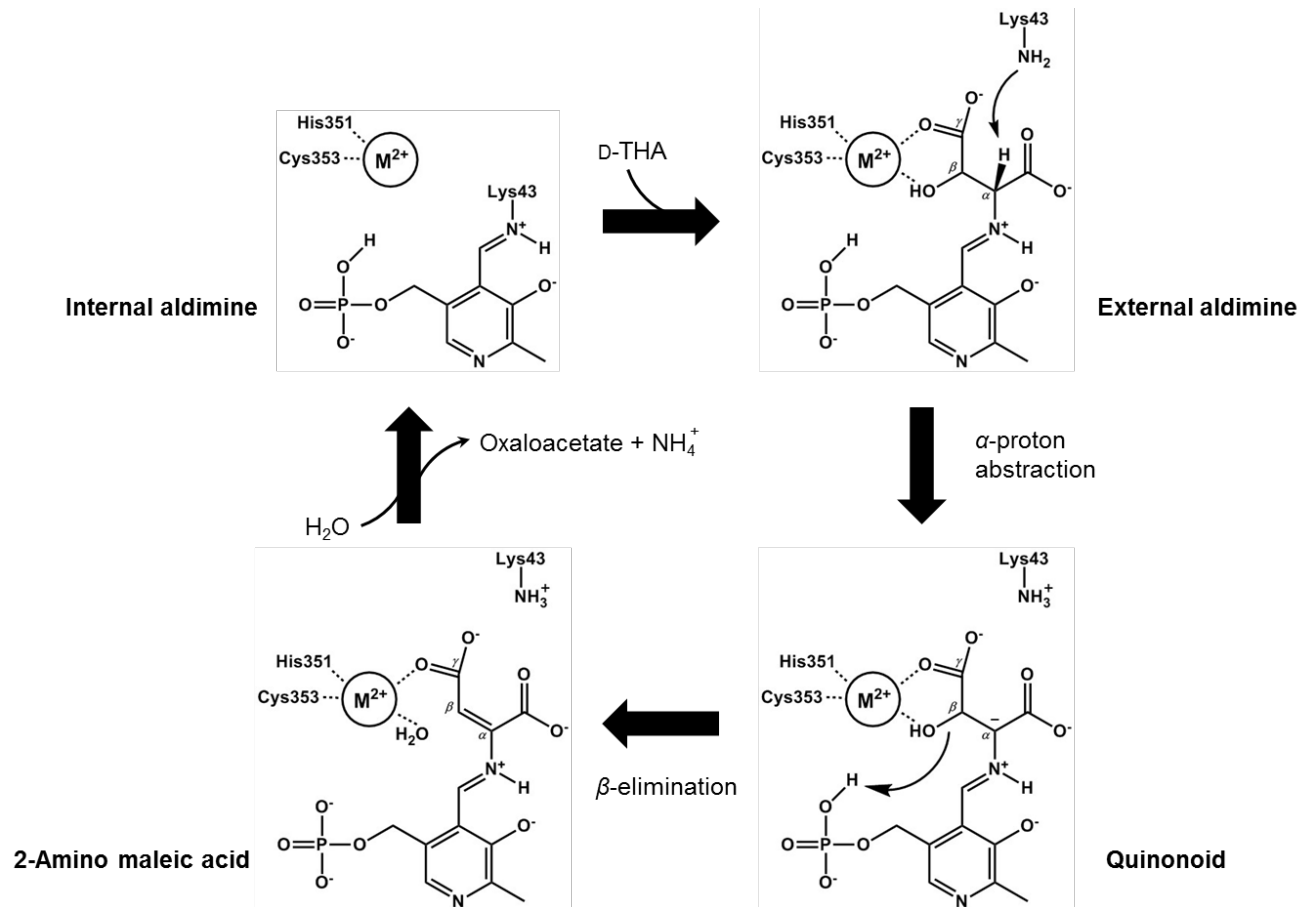


Fig. 5 Matsumoto et al.

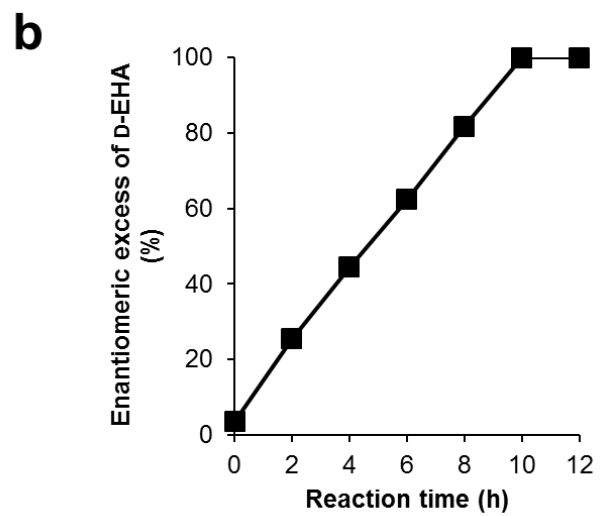
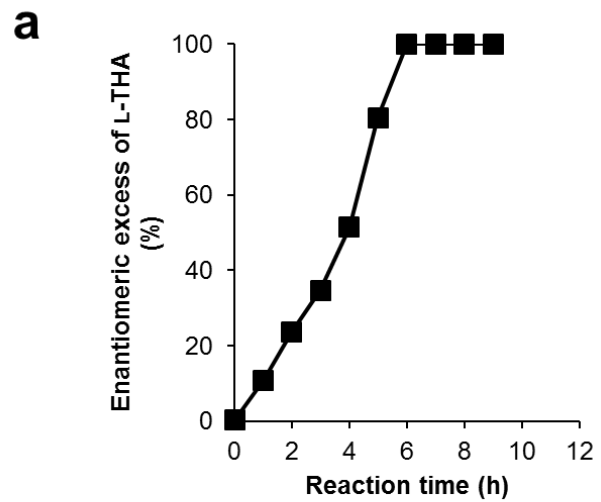


Fig. 6 Matsumoto et al.

1 **Table 1 Crystallographic parameters and model refinement statistics.**

	Wild-type	Wild-type	Wild-type	C353A	H351A	H351A	H351A
PDB code	3WQC	3WQD	3WQF	3WQG	4PB3	4PB4	4PB5
Bound metal	Mg	Mg	-	-	Mg	Mg	Mg
Substrate/inhibitor	-	D-EHA	-	-	-	2-amino maleic acid	L-EHA
Data collection							
Beam line	BL-17A	NE-3A	BL17A	BL-17A	NW-12A	NW-12A	NW-12A
Wavelength (Å)	0.98000	1.00000	0.98000	0.98000	1.00000	1.00000	1.00000
Resolution (Å)	50-1.50	50-1.50	50-2.30	50-1.55	50-1.70	50-1.80	50-1.90
	(1.53-1.50) ^a	(1.53-1.50) ^a	(2.34-2.30) ^a	(1.58-1.55) ^a	(1.73-1.70) ^a	(1.83-1.80) ^a	(1.93-1.90) ^a
Space group	<i>I</i> ₄ 22	<i>I</i> ₄ 22	<i>I</i> ₄ 22	<i>I</i> ₄ 22	<i>I</i> ₄ 22	<i>I</i> ₄ 22	<i>I</i> ₄ 22
Cell parameters (Å)	<i>a</i> = <i>b</i> = 157.7, <i>c</i> = 158.8	<i>a</i> = <i>b</i> = 157.8, <i>c</i> = 158.2	<i>a</i> = <i>b</i> = 157.8, <i>c</i> = 157.9	<i>a</i> = <i>b</i> = 158.0, <i>c</i> = 159.1	<i>a</i> = <i>b</i> = 157.6, <i>c</i> = 158.2	<i>a</i> = <i>b</i> = 157.7, <i>c</i> = 157.4	<i>a</i> = <i>b</i> = 157.6, <i>c</i> = 157.5
Unique reflections	157,557	156,137	44,400	144,006	107,707	91,233	77,555
<i>R</i> _{merge} ^b	0.089 (0.765)	0.082 (0.591)	0.112 (0.727)	0.094 (0.857)	0.059 (0.464)	0.094 (0.672)	0.087 (0.585)
Completeness (%)	100.0 (100.0)	99.6 (100.0)	100.0 (100.0)	99.8 (100.0)	100.0 (100.0)	99.6 (99.1)	100.0 (100.0)
Redundancy	14.7 (14.6)	14.5 (13.5)	14.7 (14.7)	14.6 (14.5)	14.1 (8.5)	14.9 (15.0)	14.8 (14.8)
<i>I</i> /σ (<i>I</i>)	33.6 (5.0)	37.1 (6.5)	28.6 (7.1)	29.0 (5.6)	38.3 (5.4)	29.1 (5.4)	32.1 (7.0)
Refinement							
<i>R</i> _{work} / <i>R</i> _{free} ^{c,d}	0.121/0.152	0.144/0.176	0.198/0.239	0.143/0.179	0.166/0.185	0.164/0.183	0.153/0.187
Rmsd bond length (Å)	0.026	0.026	0.018	0.025	0.026	0.025	0.025
Rmsd bond angle (°)	2.18	2.10	1.90	2.14	2.3	2.2	2.1
Average B factor (Å ²)							
Overall	21.6	24.2	40.6	23.5	22.9	21.6	22.0
Protein	20.4	23.1	40.7	22.7	22.4	21.4	21.6

PLP	15.5	17.4	34.1	17.5	16.2	16.0	16.4
Metal (active-site Mg)	14.4	18.7	-	-	13.0	25.5	30.5
Substrate/inhibitor	-	19.0	-	-	-	27.9	26.3
Waters	32.2	34.1	38.6	31.6	28.2	24.5	26.7
Ramachandran plot (%)							
Favored	92.0	92.3	91.1	91.5	91.5	92.1	91.1
Allowed	7.4	7.4	8.4	7.9	8.2	7.6	8.6
Disallowed ^e	0.6	0.3	0.5	0.6	0.3	0.3	0.3

1 ^a Values in parentheses refer to data in the highest resolution shell.

2 ^b $R_{\text{merge}} = \sum_h \sum_i |I_{h,i} - \langle I_h \rangle| / \sum_h \sum_i I_{h,i}$, where $\langle I_h \rangle$ is the mean intensity of a set of equivalent reflections.

3 ^c $R_{\text{work}} = \sum |F_{\text{obs}} - F_{\text{calc}}| / \sum F_{\text{obs}}$ for 95% of the reflection data used in the refinement. F_{obs} and F_{calc} are observed and calculated structure factor amplitudes, respectively.

4 ^d R_{free} is the equivalent of R_{work} , except that it was calculated for a randomly chosen 5% test set excluded from refinement.

5 ^e The residues found in the disallowed regions of the Ramachandran plot are Arg141, Phe241 and Ser284; all of these residues have well-defined electron density and
6 their main-chain conformations are reliable.

7

1 **Table 2 Specific activities of the wild-type and mutants of D-THA DH.**

Variant	3-Hydroxyaspartate dehydratase activity ($\mu\text{mol}/\text{min}/\text{mg}$ protein)	
	D-THA	L-EHA
Wild-type	21.1 ± 0.79 (100)	16.1 ± 0.18 (100)
H351A	0.12 ± 0.001 (0.57)	0.46 ± 0.006 (2.86)
C353A	N.D.	N.D.

2 Values in parentheses refer to the relative activity (%)

3 N.D.: not detected (less than $0.01 \mu\text{mol}/\text{min}/\text{mg}$ protein)

4

Supplementary Material for *Applied Microbiology and Biotechnology*

Structural insights into the substrate stereospecificity of D-threo-3-hydroxyaspartate dehydratase from *Delftia* sp. HT23: a useful enzyme for the synthesis of optically pure L-threo- and D-erythro-3-hydroxyaspartate

Yu Matsumoto,^a Yoshiaki Yasutake,^{b,*} Yuki Takeda,^a Tomohiro Tamura,^b Atsushi Yokota,^a and Masaru Wada^{a*}

^aLaboratory of Microbial Physiology, Research Faculty of Agriculture, Hokkaido University, Kita-9, Nishi-9, Kita-ku, Sapporo 060-8589, Japan, and ^bBioproduction Research Institute, National Institute of Advanced Industrial Science and Technology (AIST), 2-17-2-1 Tsukisamu-Higashi, Toyohira-ku, Sapporo 062-8517, Japan

*Corresponding authors

Tel: +81-11-857-8514; Fax: +81-11-857-8980; E-mail: y-yasutake@aist.go.jp

Tel: +81-11-706-4185; Fax: +81-11-706-4961; E-mail: wada@chem.agr.hokudai.ac.jp

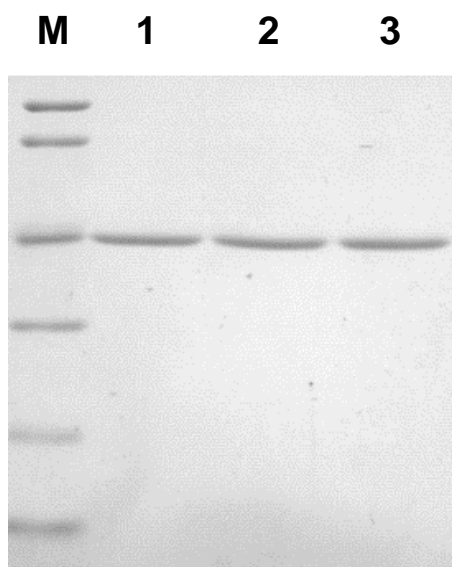


Figure S1 SDS-PAGE of the wild-type and mutants of D-THA DH. *Lanes 1-3* correspond to the wild-type, H351A, and C353A mutants, respectively. *Lane M* contains marker proteins, including (from *top* to *bottom*), phosphorylase (M_r , 97,400), bovine serum albumin (66,300), aldolase (42,400), carbonic anhydrase (30,000), trypsin inhibitor (20,100), and lysozyme (14,400). Gel was stained for protein with Coomassie Brilliant Blue R-250 (Wako Pure Chemical Industries).

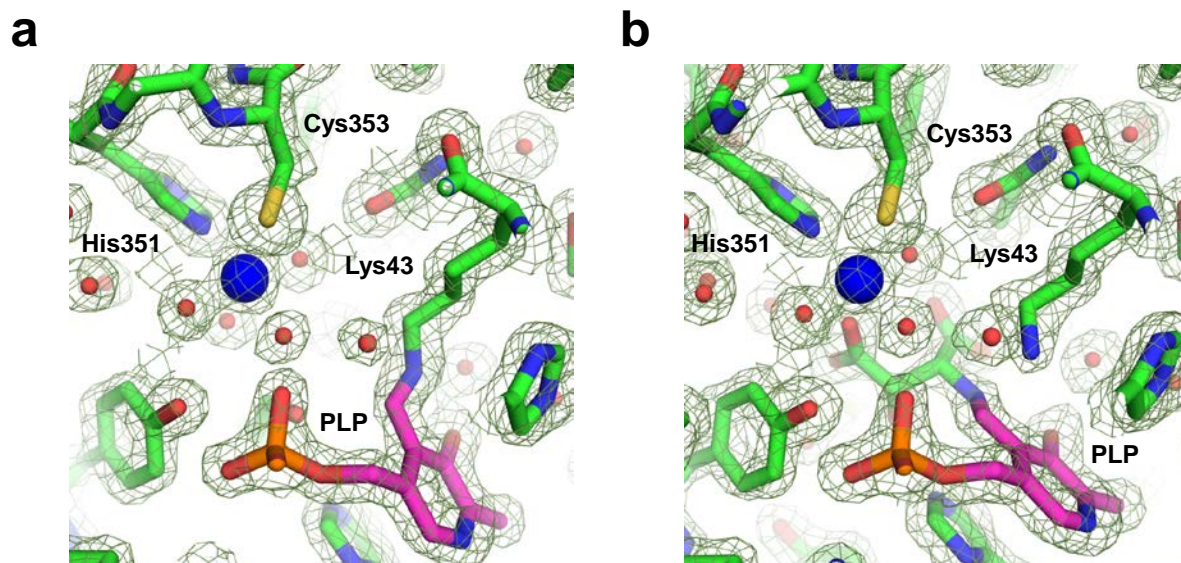


Figure S2 Final $2mF_o-DF_c$ map of the wild-type D-THA DH around active site in (a) substrate-free form (PDB code, 3WQC) and in (b) complex with D-EHA (PDB code, 3WQD), clearly showing the Schiff-base interchange from lysine-PLP to PLP-D-EHA. Each map was shows contours at 1.4σ level.

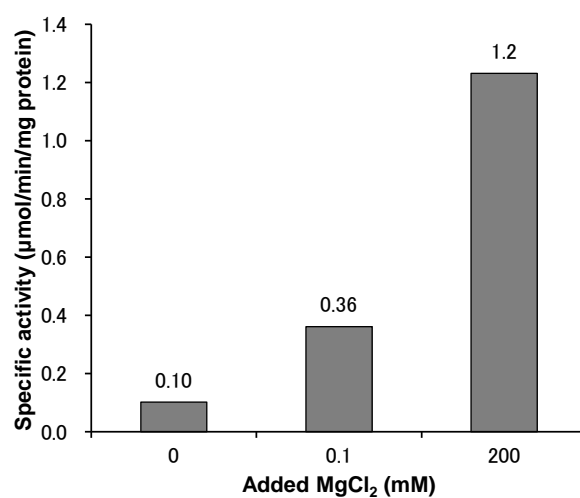


Figure S3 Effect of Mg²⁺ on the specific activity of D-THA DH. EDTA-treated enzyme was prepared using the method described earlier (Maeda et al. 2010). It was incubated for 10 min with the reaction mixture in the absence of any metal, or in the presence of 0.1 or 200 mM MgCl₂. The dehydratase activity was then measured. Addition of MgCl₂ increases the specific activity of the EDTA-treated D-THA DH.

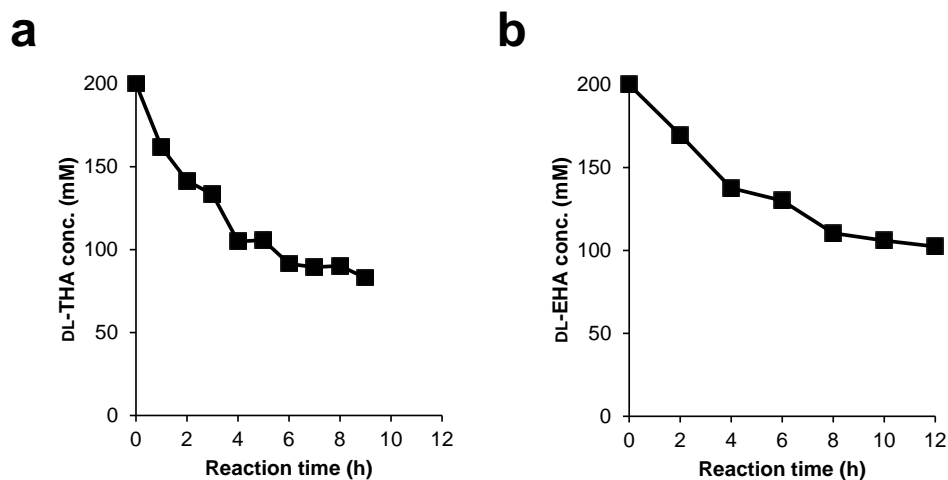


Figure S4 Time-dependent changes in the total concentration of (a) DL-THA and (b) DL-EHA in the reaction mixture. The concentration in the sample of 0 h incubation was taken as 200 mM, and the relative values for following samples were obtained. Total concentration of DL-THA and DL-EHA decreases to about half the initial value when the enantiomeric excess (*e.e.*) of L-THA and D-EHA in the reaction mixture reaches >99%, respectively.

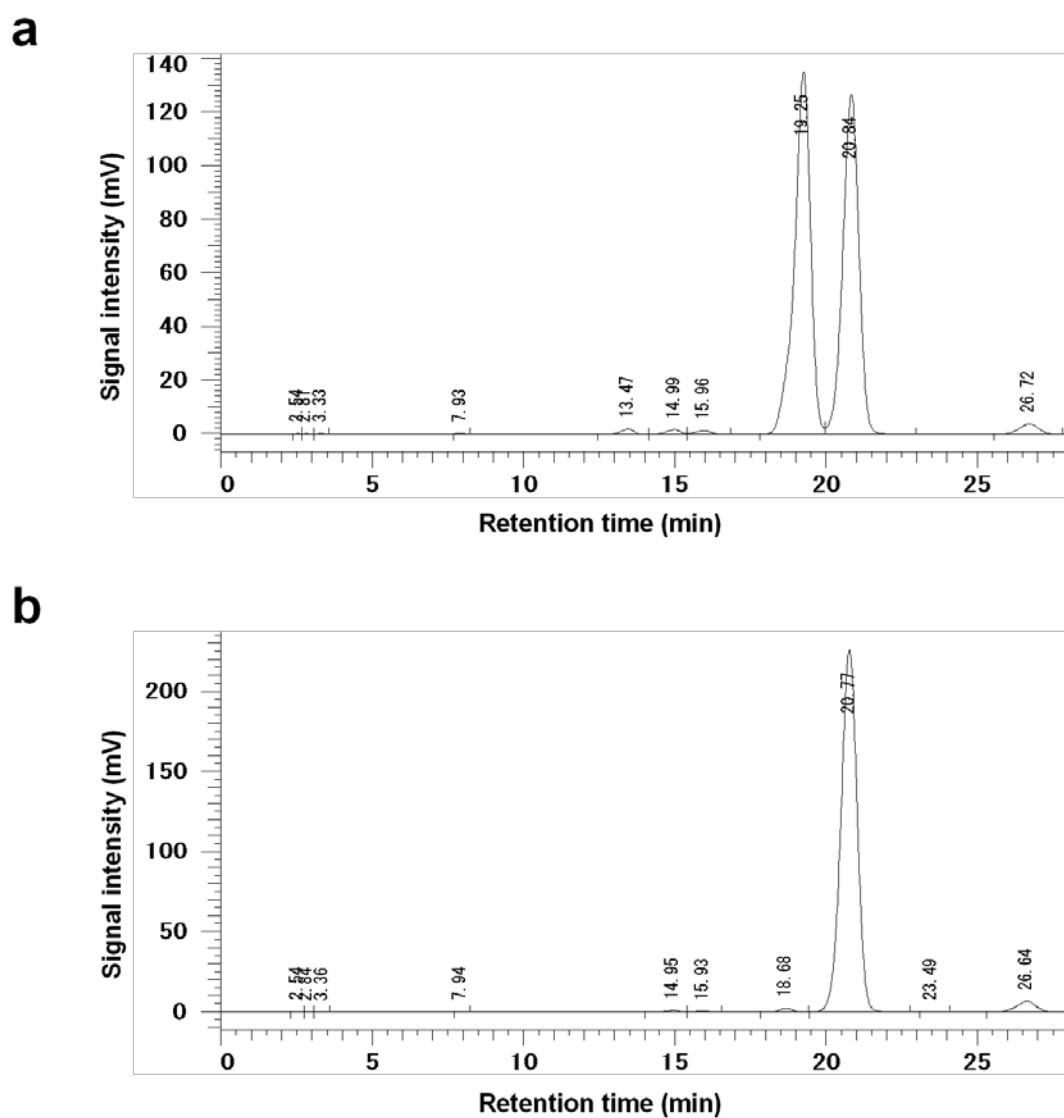
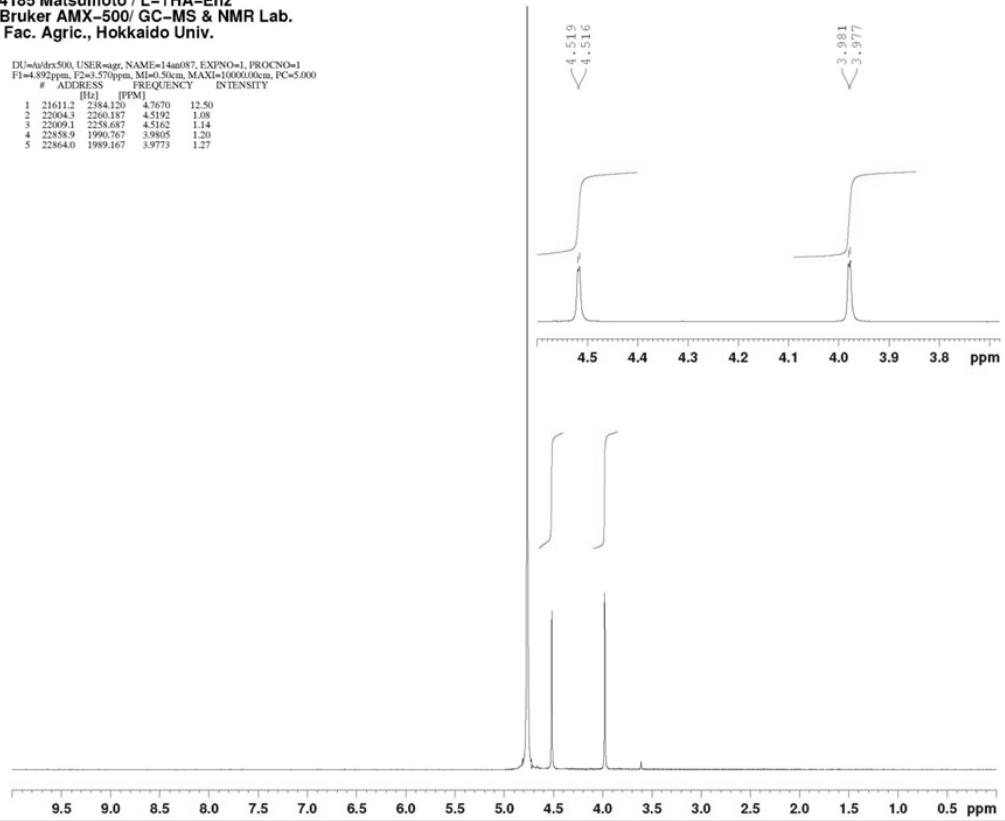


Figure S5 HPLC chromatograms recorded at 250 nm of (a) DL-THA purchased from Tokyo Chemical Industry and (b) L-THA obtained by enzymatic optical resolution. Samples were derivatized with GITC and the derivatives were analyzed using HPLC at a flow rate of 1.0 mL min⁻¹ with 30% methanol in water as the mobile phase. Retention times of the D/L-enantiomer of *threo*-3-hydroxyaspartate were 19.25/20.84 min.

a

4185 Matsumoto / L-THA-Enz
 Bruker AMX-500/ GC-MS & NMR Lab.
 Fac. Agric., Hokkaido Univ.

DU=sdex500, USER=aggr, NAME=14an087, EXPNO=1, PROCNO=1
 F1=4.892ppm, F2=3.570ppm, M1=0.50cm, MAX1=10000.00cm, PC=5.000
 # ADDRESS FREQUENCY INTENSITY
 [Hz] [PPM]
 1 21611.2 2384.120 4.7670 12.50
 2 22004.3 2260.187 4.5192 1.08
 3 22009.1 2258.687 4.5162 1.14
 4 22858.9 1990.767 3.9805 1.20
 5 22864.0 1989.167 3.9773 1.27

**b**

4185 Matsumoto / L-THA-Enz
 Bruker AMX-500/ GC-MS & NMR Lab.
 Fac. Agric., Hokkaido Univ.

DU=01, USER=aggr, NAME=14an087, EXPNO=2, PROCNO=1
 F1=232.138ppm, F2=-6.655ppm, M1=0.00cm, MAX1=13.00cm, PC=3.000
 # ADDRESS FREQUENCY INTENSITY
 [Hz] [PPM]
 1 7185.8 22607.265 179.7688 5.09
 2 7638.7 22192.152 176.4679 4.85
 3 21688.5 9316.350 74.0819 12.50
 4 23618.3 7847.786 60.0186 11.30

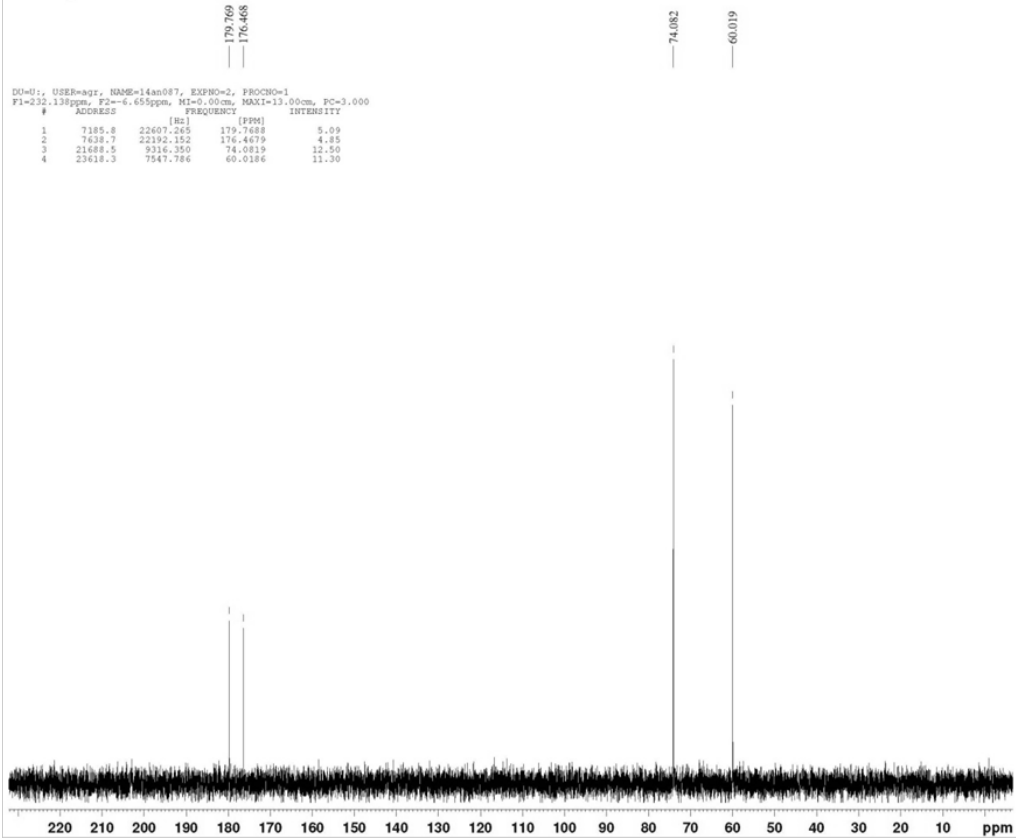


Figure S6 (a) ^1H NMR spectra recorded at 500 MHz and (b) ^{13}C NMR spectra recorded at 125 MHz of L-THA obtained by enzymatic optical resolution. Note that the ^1H signal at 4.77 ppm is attributed to deuterium oxide (D_2O).

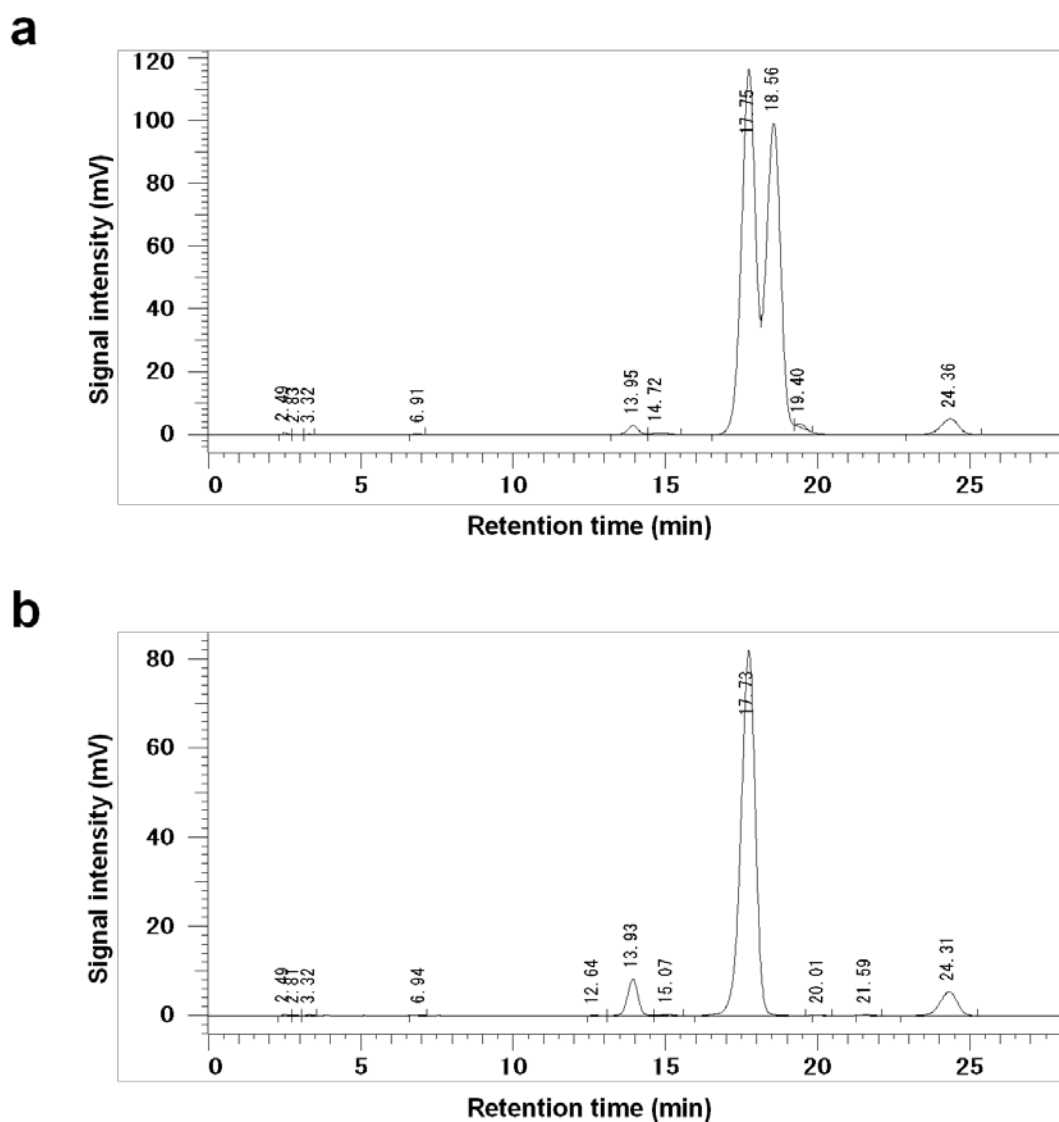
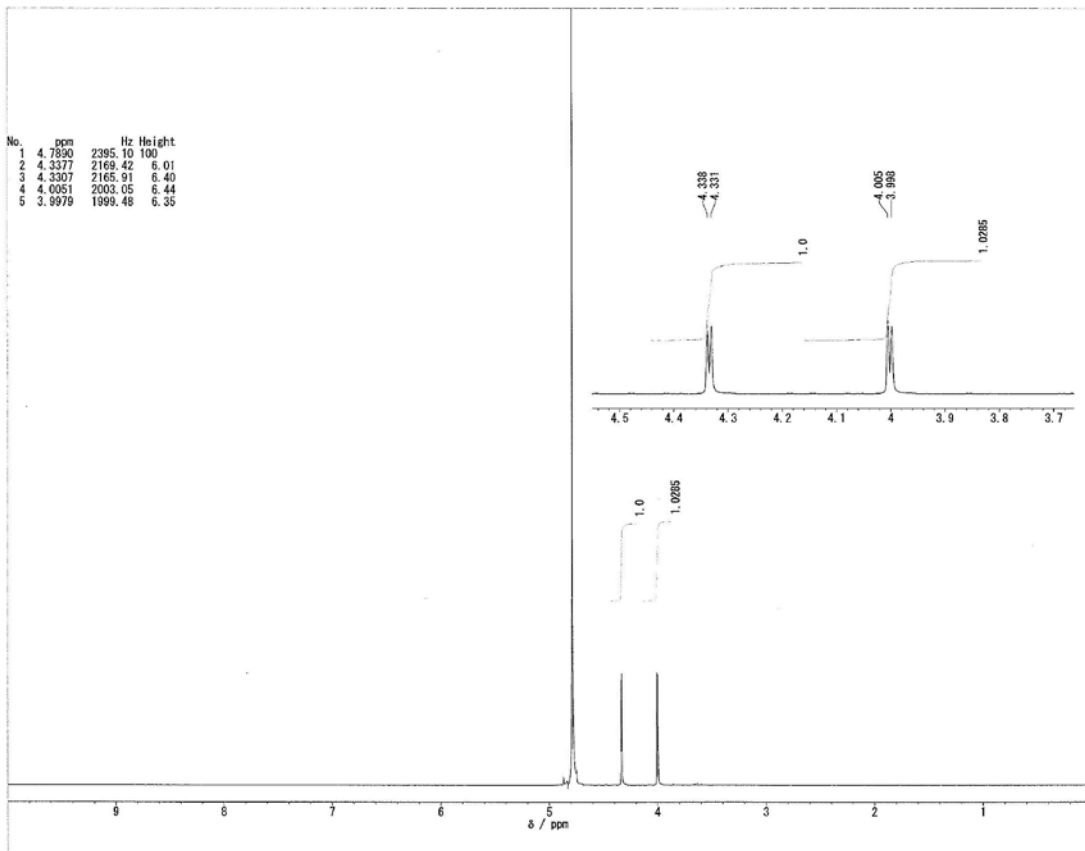


Figure S7 HPLC chromatograms recorded at 250 nm of (a) DL-EHA synthesized by the protocol described in the Materials and methods and (b) D-EHA obtained by enzymatic optical resolution. Samples were derivatized with GITC and the derivatives were analyzed using HPLC at a flow rate of 1.0 mL min^{-1} with 35% methanol in water as the mobile phase. Retention times of the D/L-enantiomer of *erythro*-3-hydroxyaspartate were 17.75/18.56 min.

a



b

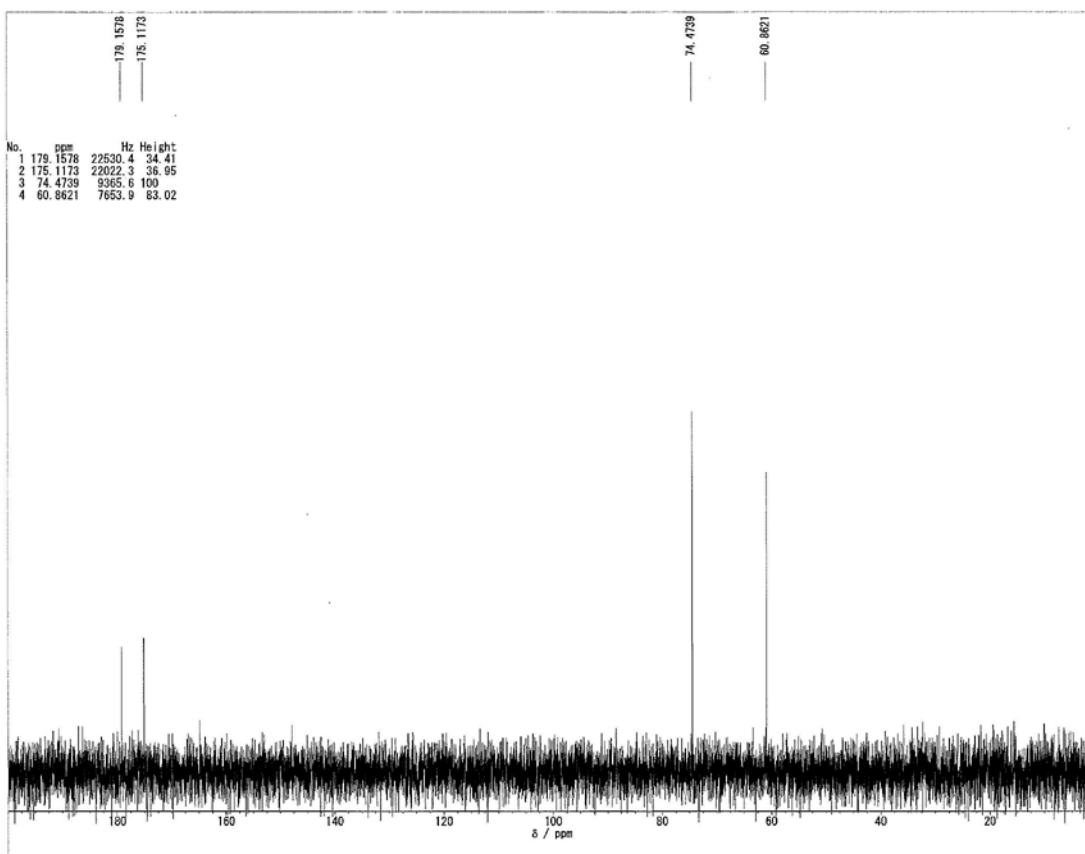


Figure S8 (a) ^1H NMR spectra recorded at 500 MHz and (b) ^{13}C NMR spectra recorded at 125 MHz of D-EHA obtained by enzymatic optical resolution. Note that the ^1H signal at 4.79 ppm is attributed to deuterium oxide (D_2O).

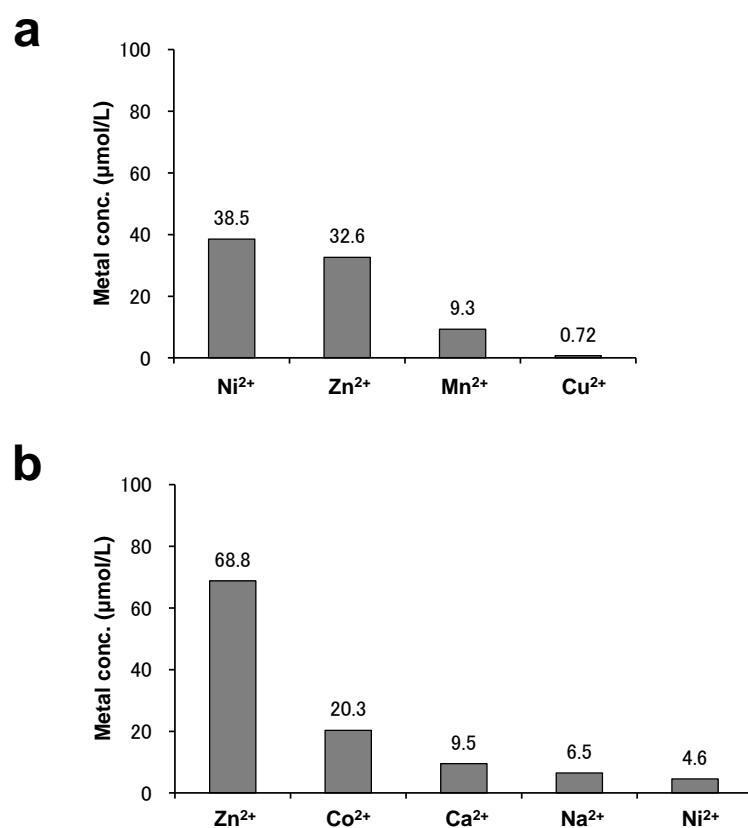


Figure S9 The metal concentration in the solution of recombinant D-THA DH purified by (a) HisTrap Ni²⁺-affinity column (GE Healthcare, Little Chalfont, UK) and (b) HisTALON Co²⁺-affinity column (Clontech Laboratories, Inc., Mountain View, CA). These were determined by inductively coupled plasma mass spectrometry (ICP-MS; ELAN DRC-e; Perkin Elmer, Waltham, MA). Enzyme concentrations were taken as 100 μmol/L. Shown are the five top-ranked metals for each analysis (Only four metals were detected in the sample of *a*). Large amount of Zn²⁺ was detected along with a relatively high content of Ni²⁺ and Co²⁺ after purification by Ni²⁺- and Co²⁺-affinity chromatography, respectively. There was a slight or no concentration of Mg²⁺.

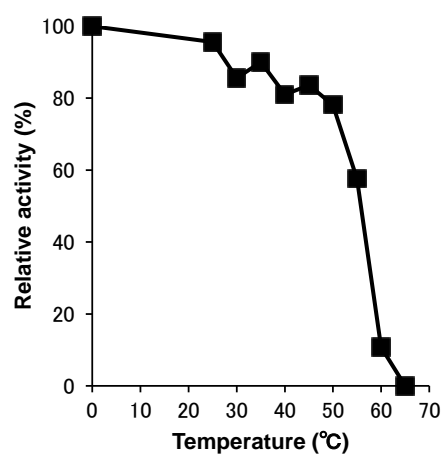


Figure S10 Thermal stability of D-THA DH. Purified D-THA DH solution was incubated for 15 min at different temperatures (0-65 °C). After incubation, it was placed on ice for 5 min and then the residual dehydratase activity was assayed by the protocol described in the Materials and methods. The activity of the enzyme incubated at 0 °C was taken as 100%. Over 80% of the residual activity was present in the range of temperature between 0 and 45 °C.